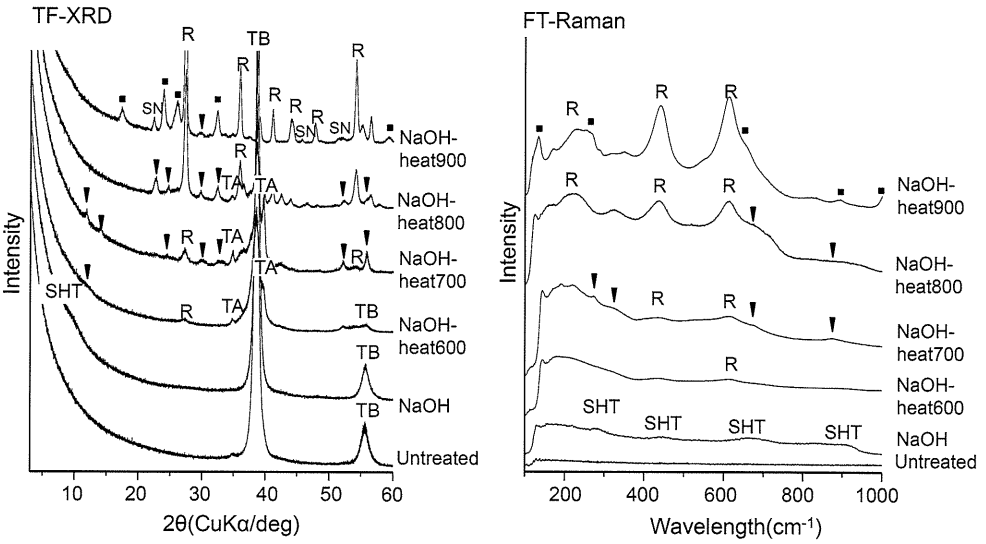

Fig. 5 TF-XRD and FT-Raman profiles of the surfaces of Ti–36Nb–2Ta–3Zr–0.3O alloy subjected to heat treatment at various temperatures after 1 M NaOH treatment. *TA* α-titanium, *TB* β-titanium, *SHT* sodium hydrogen titanate ($Na_xH_{2-x}Ti_3O_7$), *filled inverted triangle* sodium titanate ($Na_2Ti_6O_{13}$), *R* rutile, *filled square* niobium oxide (Nb_2O_5), *SN* sodium niobate ($NaNbO_3$)

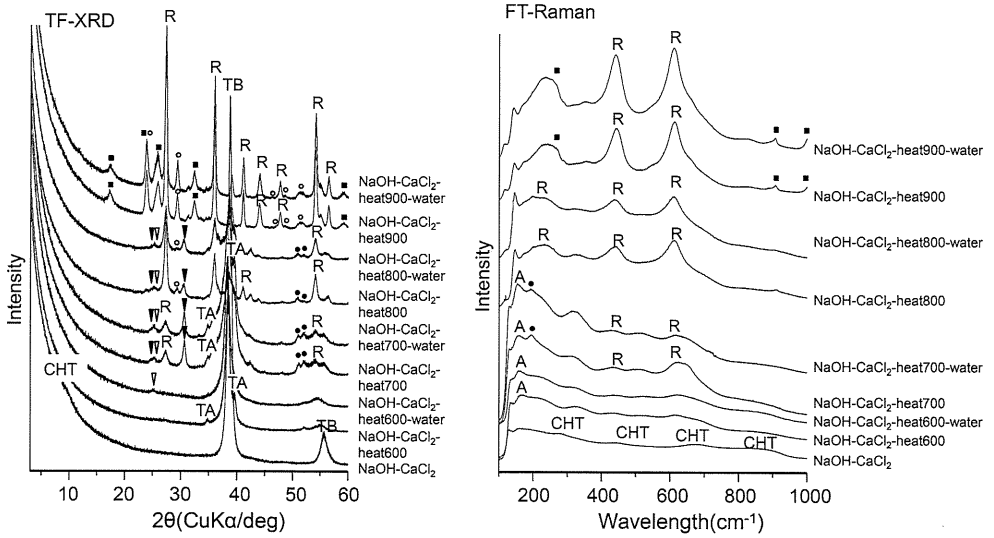

Fig. 6 TF-XRD and FT-Raman profiles of the surfaces of Ti–36Nb–2Ta–3Zr–0.3O alloy treated with 100 mM $CaCl_2$ aqueous solution after the NaOH treatment, and then subsequently subjected to heat treatment at various temperature and water treatment. *TA* α-titanium, *TB* β-titanium, *CHT* calcium hydrogen titanate ($Ca_xH_{2-2x}Ti_3O_7$), *open inverted triangle* calcium titanate ($CaTi_4O_9$), *filled inverted triangle* calcium titanate ($CaTi_2O_5$), *filled circle* calcium niobate ($CaNb_2O_7$), *open circle* calcium niobate ($CaNb_2O_6$), *filled square* niobium oxide (Nb_2O_5), *R* rutile, *A* anatase

3.2 Apatite formation

Figure 7 shows the FE-SEM photographs of the alloy surfaces soaked in SBF for 3 days after the NaOH, $CaCl_2$, heat and water treatments. It can be seen from Fig. 7 that the alloy formed spherical precipitates on their surfaces, which were identified as crystalline apatite by TF-XRD given in Fig. 8, only when subjected to the NaOH, $CaCl_2$, heat and water treatments. The amount of apatite formed on the alloy was strongly dependent on the temperature of the heat treatment, with the heat treatment at 700°C yielding the largest amount.

Figure 9 shows the FE-SEM photographs of the alloy surfaces soaked in SBF for 3 days after incubation under 95% humidity at 80°C for 1 week, following the 1 M NaOH–$CaCl_2$–heat700–water treatments. The apatite-forming ability of the treated alloy was maintained even after the incubation, indicating the long-term stability of the apatite-forming ability in a humid environment at high temperature.

3.3 Mechanical properties

Figure 10 shows the typical stress–strain curves of the rod samples of the present alloy which was untreated and subjected to the 1 M NaOH–$CaCl_2$–heat700–water treatments. It can be seen from Fig. 10 that the untreated rod samples display approximately 880 MPa of 0.2% proof

Table 2 Scratch resistance of Ti–36Nb–2Ta–3Zr–0.3O alloy subjected to 1 M NaOH, $CaCl_2$, heat at various temperature, and water treatments

Treatment	Scratch resistance (mN)	
	Average	Standard deviation
1 M NaOH	7.4	3.9
1 M NaOH–heat600	61.3	9.4
1 M NaOH–heat700	91.4	17.4
1 M NaOH–heat800	176.4	10.8
1 M NaOH–heat900	111.8	7.9
1 M NaOH–$CaCl_2$	9.3	3.1
1 M NaOH–$CaCl_2$–heat600	65.8	14.4
1 M NaOH–$CaCl_2$–heat600–water	68.7	18.0
1 M NaOH–$CaCl_2$–heat700	104.5	20.5
1 M NaOH–$CaCl_2$–heat700–water	97.1	13.7
1 M NaOH–$CaCl_2$–heat800	194.4	1.6
1 M NaOH–$CaCl_2$–heat800–water	187.6	9.5
1 M NaOH–$CaCl_2$–heat900	123.3	9.6
1M NaOH–$CaCl_2$–heat900–water	134.4	6.5

strength, 1,030 MPa of tensile strength and 11% elongation. Elastic modulus measured by free vibration method was 65.4 GPa. These mechanical properties were only a little changed by the present treatment for inducing apatite formation, that is 798 MPa of 0.2% proof strength,

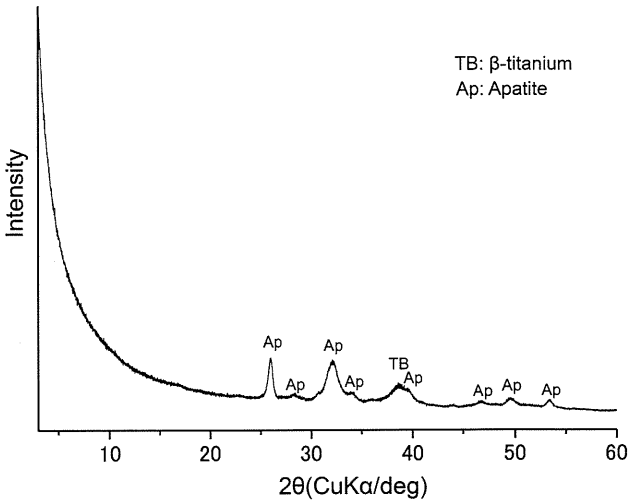

Fig. 8 TF-XRD profile of the surfaces of Ti–36Nb–2Ta–3Zr–0.3O alloy soaked in SBF for 3 days after the 1 M NaOH, $CaCl_2$, heat700 and water treatments

871 MPa of tensile strength, 10% elongation and 79.8 GPa of elastic modulus.

3.4 Microstructure

Figure 11 shows the metallurgical micrographs of the alloy samples untreated and subjected to the 1 M NaOH, $CaCl_2$,

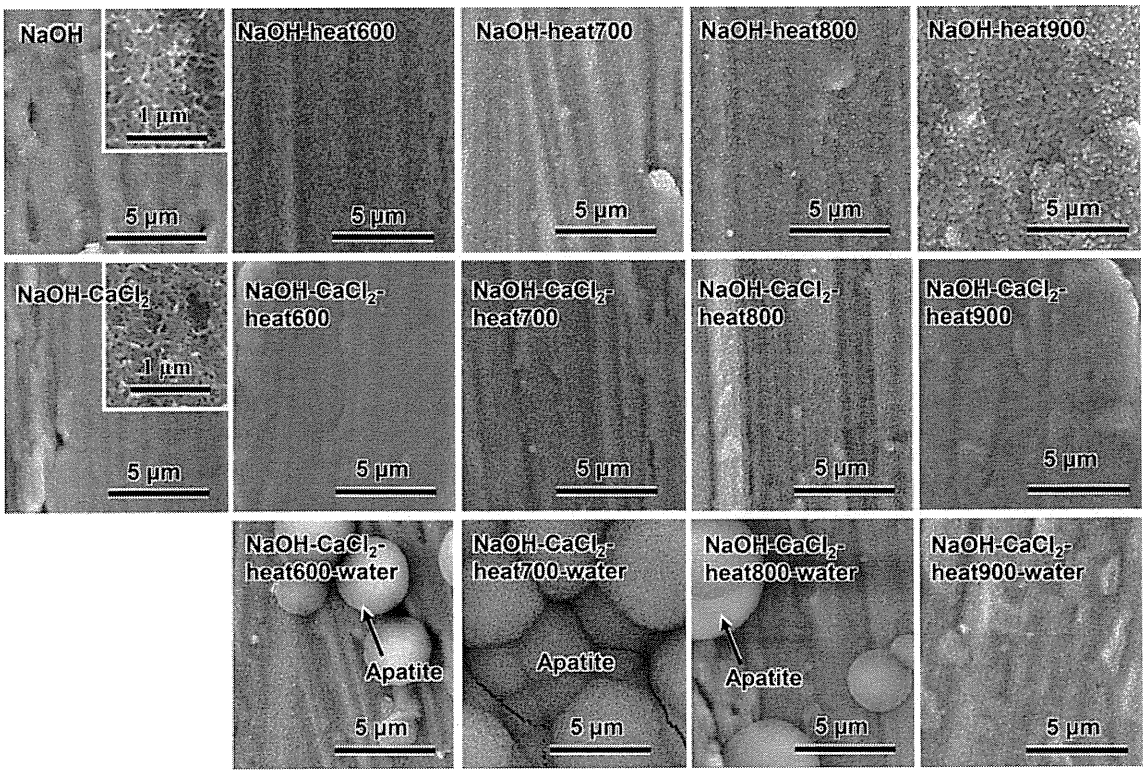

Fig. 7 FE-SEM photographs of the surfaces of Ti–36Nb–2Ta–3Zr–0.3O alloy soaked in SBF for 3 days after the NaOH, $CaCl_2$, heat at various temperatures and water treatments. *Inset* Photographs show high magnification

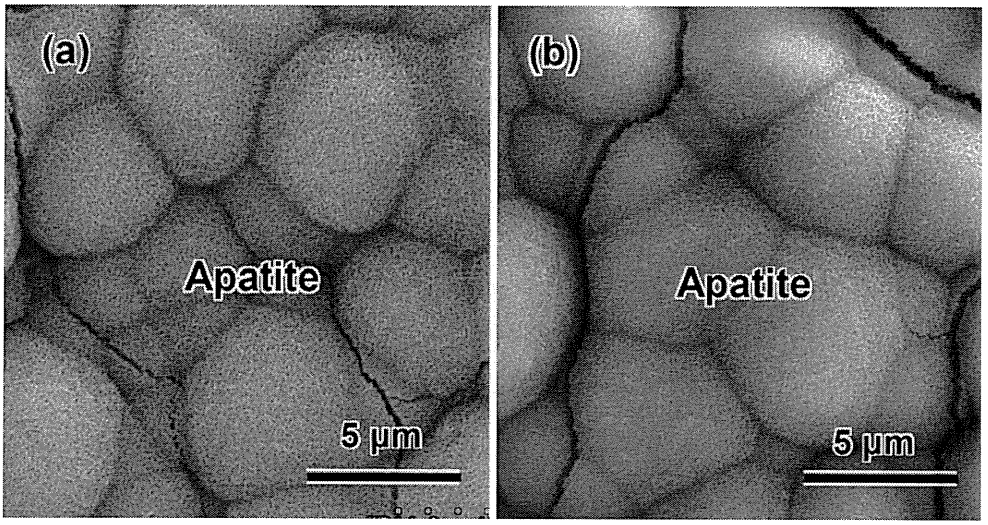

Fig. 9 FE-SEM photographs of the surfaces of Ti–36Nb–2Ta–3Zr–0.3O alloy soaked in SBF for 3 days **a** without and **b** with a storage under 95% humidity at 80°C for 1 week, following 1 M NaOH, $CaCl_2$, heat700, and water treatments

heat700 and water treatments. It can be seen from Fig. 11 that the sample took a homogeneous marble-like structure consisting of fine grains about 6 μm in width and several tens of μm in length before the treatments, while it was composed of circular large grains 10–50 μm in size accompanied by small grains after the treatments.

4 Discussion

It is apparent from Figs. 7 and 8 that high apatite formation in the Ti–36Nb–2Ta–3Zr–0.3O alloy is induced by the NaOH, $CaCl_2$, heat and water treatments, but can be induced by neither the simple NaOH plus heat treatments, nor the NaOH, $CaCl_2$ and heat treatments. The difference in the apatite-forming abilities between these surface treatments is here discussed in terms of the surface structure.

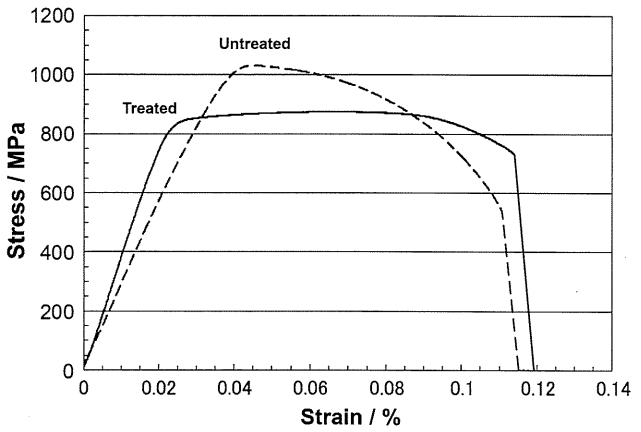

Fig. 10 Typical stress–strain curve of Ti–36Nb–2Ta–3Zr–0.3O with or without 1 M NaOH, $CaCl_2$, heat700 and water treatments

A fine network layer that was approximately 300 nm in thickness was formed on the surface of the alloy by the NaOH treatment. This network consisted of nano-sized sodium hydrogen titanate, $Na_xH_{2-x}Ti_3O_7$. When the alloy thus treated was subsequently simply heat-treated, the sodium hydrogen titanate was transformed into sodium titanate, $Na_2Ti_6O_{13}$, and rutile at temperatures lower than 800°C. These surface structural changes of the present alloy are similar to those reportedly observed in pure titanium metal due to the NaOH and heat treatments [27]. In the case of the pure Ti metal, the treated metal forms apatite on its surface in SBF by the following mechanism. The sodium ions in the sodium titanate release via exchange with oxionium ions in SBF to form Ti–OH groups on the surface of the Ti metal [31, 32]. As a result, the pH of the surrounding SBF increases. The Ti–OH groups are negatively charged in the alkali solution [33] so as to combine with the positively charged calcium ions in SBF. As the calcium ions accumulate, the surface of the Ti metal is positively charged and combines with the negatively charged phosphate ions, forming the apatite [31, 32]. The reason the present alloy with the sodium titanate on its surface did not form the apatite in SBF might be attributed to the suppression of sodium ion release from the sodium titanate by the incorporated niobium ions, as in the case of the Ti–15Zr–4Nb–4Ta alloy [15].

When the present alloy was subjected to the $CaCl_2$ treatment after the NaOH treatment, the sodium hydrogen titanate formed by the NaOH treatment substituted the sodium ions with calcium ions to form a calcium hydrogen titanate, $Ca_xH_{2-2x}Ti_3O_7$, which takes a layered structure

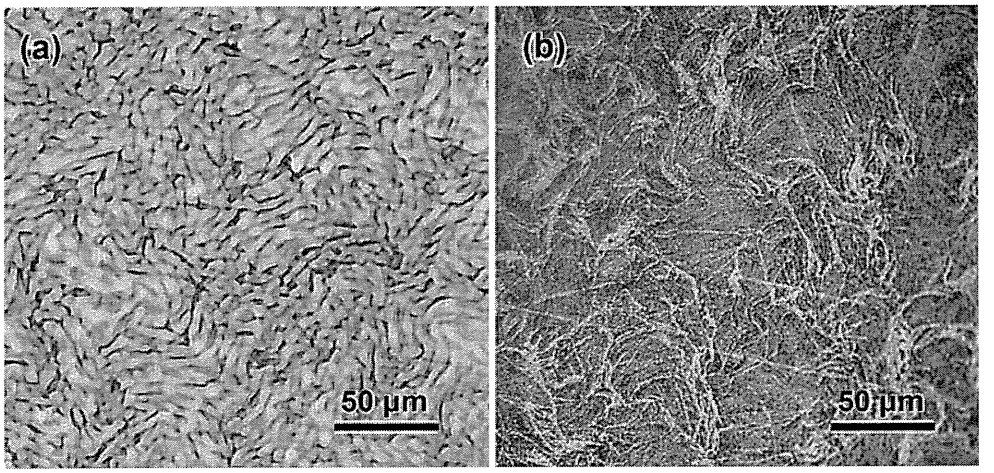

Fig. 11 Metallurgical micrographs of Ti–36Nb–2Ta–3Zr–0.3O alloy **a** untreated and **b** subjected to 1 M NaOH, $CaCl_2$, heat700 and water treatments

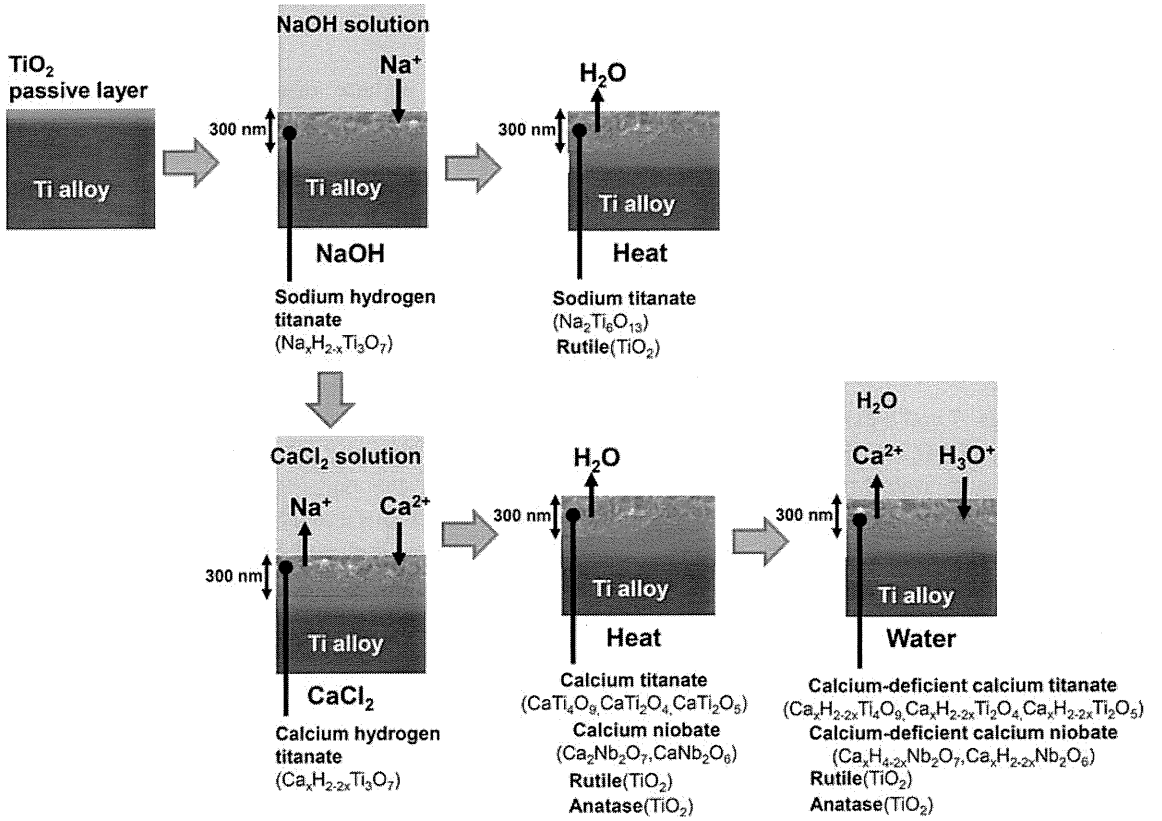

Fig. 12 Structural changes of the surfaces of Ti–36Nb–2Ta–3Zr–0.3O due to NaOH, $CaCl_2$, heat and water treatments

[34]. Thus, the formed calcium hydrogen titanate transformed into various forms of calcium titanate, such as $CaTi_4O_9$, $CaTi_2O_4$ and $CaTi_2O_5$, calcium niobate such as $Ca_2Nb_2O_7$ and $CaNb_2O_6$, rutile and anatase by the subsequent heat treatment, as is schematically shown in Fig. 12. None of the alloys treated in this manner formed apatite on their surfaces in SBF. This might be attributed to the extremely low diffusion constant of the calcium ions in the formed calcium titanates and niobate, as in the case of the calcium titanate of Ti–15Zr–4Nb–4Ta alloy [16].

The final water treatment exchanged a portion of the calcium ions in the surface layer for oxonium ions without an apparent change in the crystal phases, as shown in Figs. 4 and 6. Thus, the resultant phases can be described as $Ca_xH_{2-2x}Ti_4O_9$, $Ca_xH_{2-2x}Ti_2O_4$ and $Ca_xH_{2-2x}Ti_2O_5$ for the calcium-deficient calcium titanate, and $Ca_xH_{4-2x}Nb_2O_7$

and $Ca_xH_{2-2x}Nb_2O_6$ for the calcium-deficient calcium niobate. The alloy treated thus exhibited a high capacity for apatite formation in SBF, as shown in Fig. 7. This might be due to the increased mobility of the calcium ions in the calcium titanates and niobates by incorporation of the some amounts of oxonium ions [16]. When the calcium ions are released from the calcium titanates and niobates in SBF, they promote apatite formation not only by the same mechanism as the sodium ions described above, but also by increasing ionic activity product of the apatite by the released calcium ions themselves.

However, it should be noted that thus induced apatite-forming ability was strongly dependent on the heat treatment temperature after the $CaCl_2$ treatment. The treated alloy showed the highest apatite-forming ability when it was heat-treated at 700°C. This could be attributed to the dominant precipitation of $CaTi_2O_5$ at around 700°C, as shown in Fig. 6. The calcium ions are more condensed in this compound than other calcium titanates such as $CaTi_4O_9$, and hence are easily released in SBF.

The mobility of the calcium ions in the calcium titanate is, however, not so high that the calcium content is appreciably decreased in a humid environment. As a result, the high capacity for apatite formation conferred on the alloy by these treatments was maintained even after the incubation with 95% relative humidity at 80°C for at least 1 week. This is an important property in clinical applications, since medical devices are sometimes stored in humid condition for a long period of time before implantation.

In clinical applications, the scratch resistance of the chemically and thermally treated surface layer of the devices is also important. The experimental results described above also showed that the present alloy, after being subjected to the chemical and heat treatments so as to give high capacity for apatite formation, also exhibits high scratch resistance. It was experimentally confirmed that the high scratch resistance was maintained even after the incubation in humid condition.

It has been shown that Ti and various kinds of Ti-based alloys with the capacity to form apatite on their surfaces in SBF bond to living bone through the apatite layer formed on their surfaces in the living body [10, 11, 16, 17, 19–23]. In view of these findings, the present results indicate that the present alloy subjected to 1 M NaOH–$CaCl_2$–heat700–water treatments is likely to tightly bond to living bone in the body.

Generally, the mechanical properties of Ti-based alloys are liable to be changed by chemical and heat treatments. It can be confirmed from Fig. 10 that the favorable mechanical properties of the present alloy, such as the low elastic modulus, high mechanical strength and large elastic deformation are only a little changed by the 1 M NaOH–$CaCl_2$–heat700–water treatments. The slight decrease in the proof strength from 880 to 798 MPa and slight increase in the elastic modulus from 65.4 to 79.8 GPa might be attributed to partial phase transformation of β-Ti to α-Ti in the alloy and their grain growth by the heat treatment after the chemical treatment, as shown in Figs. 6 and 11. Regardless of these small changes, the treated alloy still possesses higher mechanical strength and lower elastic modulus, which are favorable for orthopedic and dental implants, than Ti metal and conventional Ti alloy such as Ti–6Al–4V [35].

5 Conclusion

Ti–36Nb–2Ta–3Zr–0.3O alloy exhibits a high capacity for apatite formation in SBF when it was soaked in 1 M NaOH and 100 mM $CaCl_2$ solutions, heat-treated at 700°C, and soaked in water at 80°C. The first NaOH treatment forms sodium hydrogen titanate on the surface of the alloy, which serves as a precursor from which calcium hydrogen titanate is derived in the second $CaCl_2$ treatment. The third heat treatment transforms the calcium hydrogen titanate into calcium titanate predominately $CaTi_2O_5$ which exhibits high apatite formation in SBF after the subsequent hot water treatment which exchanges a portion of the calcium ions with oxionium ions. Thus, this capacity for high apatite formation was maintained even when the treated alloy was stored in a humid environment for a long period. The treated alloy also possesses a high level of scratch resistance, which is useful for clinical application. The sequential treatment in the present study consists of simple solution and heat treatments, which does not need any special and expensive apparatus, and is easily applied to large devices with complicated shapes. These features will be favorable for commercial manufacture.

The favorable mechanical properties of the present alloy, such as low elastic modulus, high mechanical strength and extensive elastic deformation are little changed by the surface treatment for inducing the apatite-forming ability. The present alloy conferred with high capacity for apatite formation is believed to be useful as unique materials for orthopedic and dental implants, since the treated alloy is expected to tightly bonds to bone in the living body and exhibit favorable mechanical properties.

References

1. Kokubo T, Miyaji F, Kim HM, Nakamura T. Spontaneous formation of bone-like apatite layer on chemically treated titanium metal. J Am Ceram Soc. 1996;79:1127–9.
2. Yan QW, Nakamura T, Kobayashi M, Kim HM, Kokubo T. Bonding of chemically treated titanium implants to bone. J Biomed Mater Res. 1997;37:267–75.

3. Wang XX, Hayakawa S, Tsuru K, Osaka A. Bioactive titania gel layers formed by chemical treatment of Ti substrate with a H_2O_2/HCl solution. Biomaterials. 2002;23:1353–7.
4. Wang XX, Yan W, Hayakawa S, Tsuru K, Osaka A. Apatite deposition on thermally and anodically oxidized titanium surfaces in a simulated body fluid. Biomaterials. 2003;24:4631–7.
5. Wu JM, Hayakawa S, Tsuru K, Osaka A. Low-temperature preparation of anatase and rutile layers on titanium substrates and their ability to induce in vitro apatite deposition. J Am Ceram Soc. 2004;87:1635–42.
6. Lu X, Wang Y, Yang X, Zhang Q, Zhao Z, Weng LT, Leng Y. Spectroscopic analysis of titanium surface functional groups under various surface modification and their behaviors in vitro and in vivo. J Biomed Mater Res. 2008;84A:523–34.
7. Sugino A, Ohtsuki C, Tsuru K, Hayakawa S, Nakano T, Okazaki Y, Osaka A. Effect of spatial design and thermal oxidation on apatite formation on Ti–15Zr–4Ta–4Nb alloy. Acta Biomater. 2009;5:298–304.
8. Karthega M, Rajendran N. Hydrogen peroxide treatment on Ti–6Al–4V alloy: a promising surface modification technique for orthopaedic application. Appl Surf Sci. 2010;256:2176–83.
9. Kawanabe K, Ise K, Goto K, Akiyama H, Nakamura T, Kaneuji A, Sugimori T, Mtsumoto T. Clinical device-related article a new cementless total hip arthroplasty with bioactive titanium porous-coating by alkaline and heat treatment: average 4.8-year results. J Biomed Mater Res Part B. 2009;90B:476–81.
10. Kim HM, Miyaji F, Kokubo T, Nakamura T. Preparation of bioactive Ti and its alloy via simple chemical surface treatment. J Biomed Mater Res. 1996;32:409–17.
11. Nishiguchi S, Nakamura T, Kobayashi M, Kim HM, Miyaji F, Kokubo T. Enhancement of bone-bonding strengths of titanium alloy implants by alkali and heat treatments. J Biomed Mater Res (Appl Biomater). 1999;48:689–96.
12. Geetha M, Singh AK, Asokamani R, Gogia AK. Ti based biomaterials, the ultimate choice for orthopedic implants—a review. Prog Mater Sci. 2009;54:397–425.
13. Kawahara H, Ochi S, Tanetani K, Kato K, Isogai M, Mizuno H, et al. Biological testing of dental materials. J Jpn Soc Dent Appar Mater. 1963;4:65–75.
14. Okazaki Y, Rao S, Ito Y, Tateishi T. Corrosion resistance, mechanical properties, corrosion fatigue strength and cytocompatibility of new Ti alloys without Al and V. Biomaterials. 1998;19:1197–215.
15. Yamaguchi S, Takadama H, Matsushita T, Nakamura T, Kokubo T. Preparation of bioactive Ti–15Zr–4Nb–4Ta alloy from HCl and heat treatments after an NaOH treatment. J Biomed Mater Res Part A. 2011;97A:135–44.
16. Yamaguchi S, Takadama H, Matsushita T, Nakamura T, Kokubo T. Apatite-forming ability of Ti–15Zr–4Nb–4Ta alloy induced by calcium solution treatment. J Mater Sci Mater Med. 2010;21:439–44.
17. Fukuda A, Takemoto M, Saito T, Fujibayashi S, Neo M, Yamaguchi S, Kizuki T, Matsushita T, Niinomi M, Kokubo T, Nakamura T. Bone bonding bioactivity of Ti metal and Ti–Zr–Nb–Ta alloys with Ca ions incorporated on their surfaces by simple chemical and heat treatments. Acta Biomater. 2011;7:1379–86.
18. Saito T, Furuta T, Hwang JH, Kuramoto S, Nishino K, Suzuki N, Chen R, Yamada A, Ito Kazuhiko, Seno Y, Nonaka T, Ikehata H, Nagasako N, Iwamoto C, Ikuhara Y, Sakuma T. Multifunctional alloys obtained via a dislocation-free plastic deformation mechanism. Science. 2003;300:464–7.
19. Kim HM, Takadama H, Miyaji F, Kokubo T, Nishiguchi S, Nakamura T. Formation of bioactive functionally graded structure on Ti–6Al–4V alloy by chemical surface treatment. J Mater Sci Mater Med. 2000;11:555–9.
20. Kim HM, Takadama H, Kokubo T, Nishiguchi S, Nakamura T. Formation of a bioactive graded surface structure on Ti–15Mo–5Zr–3Al alloy by chemical treatments. Biomaterials. 2000;21:353–8.
21. Kizuki T, Takadama H, Matsushita T, Nakamura T, Kokubo T. Preparation of bioactive Ti metal surface enriched with calcium ions by chemical treatment. Acta Biomater. 2010;6:2836–42.
22. Nishiguchi S, Fujibayashi S, Kim HM, Kokubo T, Nakamura T. Biology of alkali- and heat- treated titanium implants. J Biomed Mater Res. 2003;67A:26–35.
23. Kokubo T, Pattanayak DK, Yamaguchi S, Takadama H, Matsushita M, Kawai T, Takemoto M, Fujibayashi S, Nakamura T. Positively charged bioactive Ti metal prepared by simple chemical and heat treatments. J R Soc Interface. 2010;7:S503–13.
24. Yamaguchi S, Takadama T, Matsushita T, Nakamura T, Kokubo T. Cross-sectional analysis of the surface ceramic layer developed on Ti metal by NaOH-heat treatment and soaking in SBF. J Ceram Soc Jpn. 2009;117:1126–30.
25. Kokubo T, Takadama H. How useful is SBF in predicting in vivo bone bioactivity? Biomaterials. 2006;27:2907–15.
26. Sun X, Li Y. Synthesis and characterization of ion-exchangeable titanate nanotubes. Chem Eur J. 2003;9:2229–38.
27. Kawai T, Kizuki T, Takadama H, Matsushita T, Kokubo T, Unuma H, Nakamura T. Apatite formation on surface titanate layer with different Na content on Ti metal. J Ceram Soc Jpn. 2010;9:19–24.
28. Joint Committee on Powder Diffraction Standards (JCPDS) Powder Diffraction Data File 00-026-0333.
29. Joint Committee on Powder Diffraction Standards (JCPDS) Powder Diffraction Data File 01-072-1134.
30. Joint Committee on Powder Diffraction Standards (JCPDS) Powder Diffraction Data File 00-025-1450.
31. Kim HM, Himeno T, Kawashita M, Lee JH, Kokubo T, Nakamura T. Surface potential change in bioactive titanium metal during the process of apatite formation in simulated body fluid. J Biomed Mater Res. 2003;67A:1305–9.
32. Takadama H, Kim HM, Kokubo T, Nakamura T. TEM-EDX Study of mechanism of bonelike apatite formation on bioactive titanium metal in simulated body fluid. J Biomed Mater Res. 2001;57:441–8.
33. Textor M, Sitting C, Franchiger V, Tosatti S, Brunette DM. Properties and biological significance of natural oxide films on titanium and its alloys. In: Brunette DM, Tengrall P, Textor M, Thomsen P, editors. Tianium in medicine. New York: Springer; 2001. p. 172–230.
34. Morgado E Jr, de Abreu MAS, Pravia ORC, Marinkovic BA, Jardim PM, Rizzo FC, Aroújo AS. A study on the structure and thermal stability of titanate nanotubes as a function of sodium content. Solid State Sci. 2006;8:888–900.
35. The Japan Institute of Metal. Metal data book: a fourth look. Tokyo: Maruzen; 2004: p. 256.

JOURNAL OF THE ROYAL SOCIETY Interface

Apatite-forming ability of titanium in terms of pH of the exposed solution

Deepak K. Pattanayak, Seiji Yamaguchi, Tomiharu Matsushita, Takashi Nakamura and Tadashi Kokubo

J. R. Soc. Interface published online 14 March 2012
doi: 10.1098/rsif.2012.0107

JOURNAL OF THE ROYAL SOCIETY Interface

FirstCite® e-publishing

J. R. Soc. Interface
doi:10.1098/rsif.2012.0107
Published online

Apatite-forming ability of titanium in terms of pH of the exposed solution

Deepak K. Pattanayak[1], Seiji Yamaguchi[1], Tomiharu Matsushita[1], Takashi Nakamura[2] and Tadashi Kokubo[1,*]

[1]*Graduate School of Biomedical Sciences, Chubu University, 1200 Matsumoto-cho, Kasugai 487-8501, Japan*
[2]*Kyoto Medical Center, National Hospital Organisation, 1-1, Fukakusa Mukaihata-cho, Fushimi-ku, Kyoto 612-8555, Japan*

In order to elucidate the main factor governing the capacity for apatite formation of titanium (Ti), Ti was exposed to HCl or NaOH solutions with different pH values ranging from approximately 0 to 14 and then heat-treated at 600°C. Apatite formed on the metal surface in a simulated body fluid, when Ti was exposed to solutions with a pH less than 1.1 or higher than 13.6, while no apatite formed upon exposure to solutions with an intermediate pH value. The apatite formation on Ti exposed to strongly acidic or alkaline solutions is attributed to the magnitude of the positive or negative surface charge, respectively, while the absence of apatite formation at an intermediate pH is attributed to its neutral surface charge. The positive or negative surface charge was produced by the effect of either the acidic or alkaline ions on Ti, respectively. It is predicted from the present results that the bone bonding of Ti depends upon the pH of the solution to which it is exposed, i.e. Ti forms a bone-like apatite on its surface in the living body and bonds to living bone through the apatite layer upon heat treatment after exposure to a strongly acidic or alkaline solution.

Keywords: titanium; NaOH or HCl treatments; apatite-forming ability; simulated body fluid; zeta potential; X-ray photoelectron spectroscopy

1. INTRODUCTION

Titanium (Ti) and its alloys are widely used in various types of implants in orthopaedic and dental fields, because of their good biocompatibility and high mechanical strength [1]. It is reported that they could have bonded to living bone after long-term implantation. However, they do not always bond to living bone, especially in a short period of time after implantation [2] and hence, their fixation in the living body is not always stable. Fast and reliable bonding to the bone is desirable for orthopaedic and dental implants. Various attempts have been made to induce bone bonding by techniques such as ion implantation [3–5], electrochemical [6–10] and hydrothermal treatment [11–15]. Certain chemical and heat treatments have also been attempted [16–21]. Improvement in bone bonding has been reportedly induced by these treatments. However, some reports have attributed the improvement to the surface roughness increased by the treatments, while others have pointed to the formation of specific crystalline phases such as anatase and rutile induced by the treatments. There is thus inadequate consistency in these interpretations, and the purpose of the present paper is to inquire into the main factor governing the bone-bonding properties of Ti.

*Author for correspondence (kokubo@isc.chubu.ac.jp).

We previously reported that Ti and its alloys spontaneously tightly bond to living bone when soaked in NaOH solution and then subjected to heat treatment [22–24]. These treatments have been applied to a porous Ti metal layer of an artificial hip joint, and the resulting bioactive hip joint has been used clinically in Japan since 2007 [25]. On the other hand, it was also shown that Ti spontaneously bonds to living bone when soaked in a H_2SO_4/HCl mixed acid solution and then subjected to heat treatment [26]. The bonding of the Ti subjected to NaOH and acid treatments to living bone has been attributed to surface apatite formation in the living body [24,26]. However, the dependence of this apatite formation on Ti metal upon the pH of the exposed solution has not been reported.

In the present study, Ti was exposed to simple aqueous solutions in which the pH was systematically changed from approximately 0 to 14 by HCl and NaOH solutions, and then subjected to a heat treatment. Surface apatite formation was examined in a simulated body fluid (SBF) using an ion concentration almost equal to that in human blood plasma [27], in comparison with those on Ti prior to heat treatment. The dependence of their apatite-forming ability on the pH of the solution is discussed in terms of surface roughness, the kind of the surface crystalline phase and the surface charges.

It has been shown that various kinds of bone-bonding bioactive ceramics have the capacity to form

Received 9 February 2012
Accepted 23 February 2012

Table 1. pH of exposed solution.

	HCl					NaOH			
solution	5 M	1 M	100 mM	0.5 mM	water	0.5 mM	100 mM	1 M	5 M
pH	approx. 0	0.1	1.1	3.4	6–7	10.8	12.9	13.6	approx. 14

a surface apatite layer in SBF and to bond to living bone through this surface apatite layer *in vivo* [27]. The bone-bonding properties of Ti are discussed in terms of apatite-forming ability.

2. MATERIAL AND METHODS

2.1. Preparation of the samples

Commercially pure Ti (Grade no. 2; Kobe Steel, Ltd, Japan) was cut into rectangular samples having the dimensions of $10 \times 10 \times 1\ mm^3$, abraded with a no. 400 diamond plate, washed with acetone, 2-propanol and ultra pure water for 30 min each in an ultrasonic cleaner and then dried overnight in an oven at 40°C. Each specimen was soaked in 5 ml of HCl or NaOH solution at concentrations ranging from 0.5 mM to 5 M and water at 60°C in an oil bath, shaken at 120 strokes min^{-1} for 24 h, and then washed with flowed ultra-pure water for 30 s. The washing time was carefully selected as the shortest time when any precipitations from surplus NaOH solution could not be detected on the specimen treated with the NaOH solution. The pH values of the solutions are given in table 1. The specimens removed from the solutions were heated to 600°C at a rate of 5°C min^{-1} in an Fe–Cr electric furnace under an ambient atmosphere, maintained at this temperature for 1 h and then cooled naturally to room temperature in the furnace.

2.2. Surface analysis of the treated Ti metals

The surface of the Ti specimens treated as described in §2.1 was analysed using thin-film X-ray diffraction (TF-XRD, RINT-2500, Rigaku Co., Japan). The X-ray source was CuKα, and the angle of the incident beam was set to 1° against the sample surface.

The same surface was coated with a Pt/Pd film and observed under field emission scanning electron microscopy (FE-SEM, Hitachi S-4300, Hitachi, Japan).

The depth profiles of various elements near the surface of the Ti specimens subjected to the acid and heat treatments were analysed using radio frequency (RF) glow discharge optical emission spectroscopy (GD-OES, GD-Profiler 2, Horiba Co., Japan) under Ar sputtering at an Ar pressure of 600 Pa. An RF electric field with a power of 35 W was applied at a regular interval of 20 ms.

Ti plates having the dimensions of $13 \times 33 \times 1\ mm^3$ were prepared for measurement of the zeta potential, where the volume of the NaOH and HCl solutions and water for the surface treatments was increased to 20 ml. The Ti specimens soaked in the solutions and then heat-treated were electrically grounded to discharge any stray charges, and were immediately placed in the zeta potential and particle size analyser (ELS-Z1, Otsuka Electronics Co., Japan) using a glass cell for the plate sample. The zeta potential of the specimens was measured under an applied voltage of 40 V in 10 or 50 mM NaCl solution dispersing monitor particles of polystyrene latex particles (diameter = 500 nm) coated with hydroxyl propyl cellulose. When 40 V of the voltage was applied, the flow of electro-osmosis depending on the surface charge of the specimens was generated. The zeta potential was calculated from the distribution of the flow of electro-osmosis by monitoring the migration velocity of the monitor particles. Five samples were measured for each experimental condition, and the average value was used in the analysis.

2.3. Examination of the apatite formation in an simulated body fluid

The Ti specimens treated as described earlier were soaked in 30 ml of an acellular SBF at 36.5°C with ion concentrations ($Na^+ = 142.0$, $K^+ = 5.0$, $Mg^{2+} = 1.5$, $Ca^{2+} = 2.5$, $Cl^- = 147.8$, $HCO_3^- = 4.2$, $HPO_4^{2-} = 1.0$, and $SO_4^{2-} = 0.5$ mM) nearly equal to those in human blood plasma. The SBF was prepared by dissolving reagent-grade NaCl, $NaHCO_3$, KCl, $K_2HPO_4 \cdot 3H_2O$, $MgCl_2 \cdot 6H_2O$, $CaCl_2$ and Na_2SO_4 (Nacalai Tesque Inc., Japan) in ultra-pure water, and buffered at pH = 7.40 using tris (hydroxymethyl) aminomethane $[(CH_2OH)_3CNH_2]$ and 1 M HCl (Nacalai Tesque Inc.) [27].

After soaking in the SBF for 3 days, the surface was analysed for apatite formation with TF-XRD and FE-SEM using the methods described in §2.2.

The surfaces of the Ti specimens treated as described in §2.1 and soaked in SBF for various periods were analysed using X-ray photoelectron spectroscopy (XPS, ESCA-3300KM, Shimadzu Co., Japan), with MgKα radiation ($\lambda = 9.8903$ Å) as the X-ray source. The XPS take-off angle was set at 45°, which enabled the system to detect photoelectrons to a depth of 5–10 nm from the surface of the substrate. The binding energy of the measured spectra was calibrated by reference to the C_{1S} peak of the surfactant CH_2 groups on the substrate occurring at 284.6 eV.

3. RESULTS

3.1. Surface structure of the treated Ti metal

Figure 1 shows the FE-SEM micrographs of the surface of Ti specimens exposed to solutions with the different pHs, and also those that were subsequently heat-treated. Cross-sectional photographs of the Ti specimens exposed to solutions with the low or high pHs and subsequently heat-treated are also shown. It can be seen from figure 1 that a ripple-like micrometre scale roughness was formed on the Ti surface by exposure to solutions with

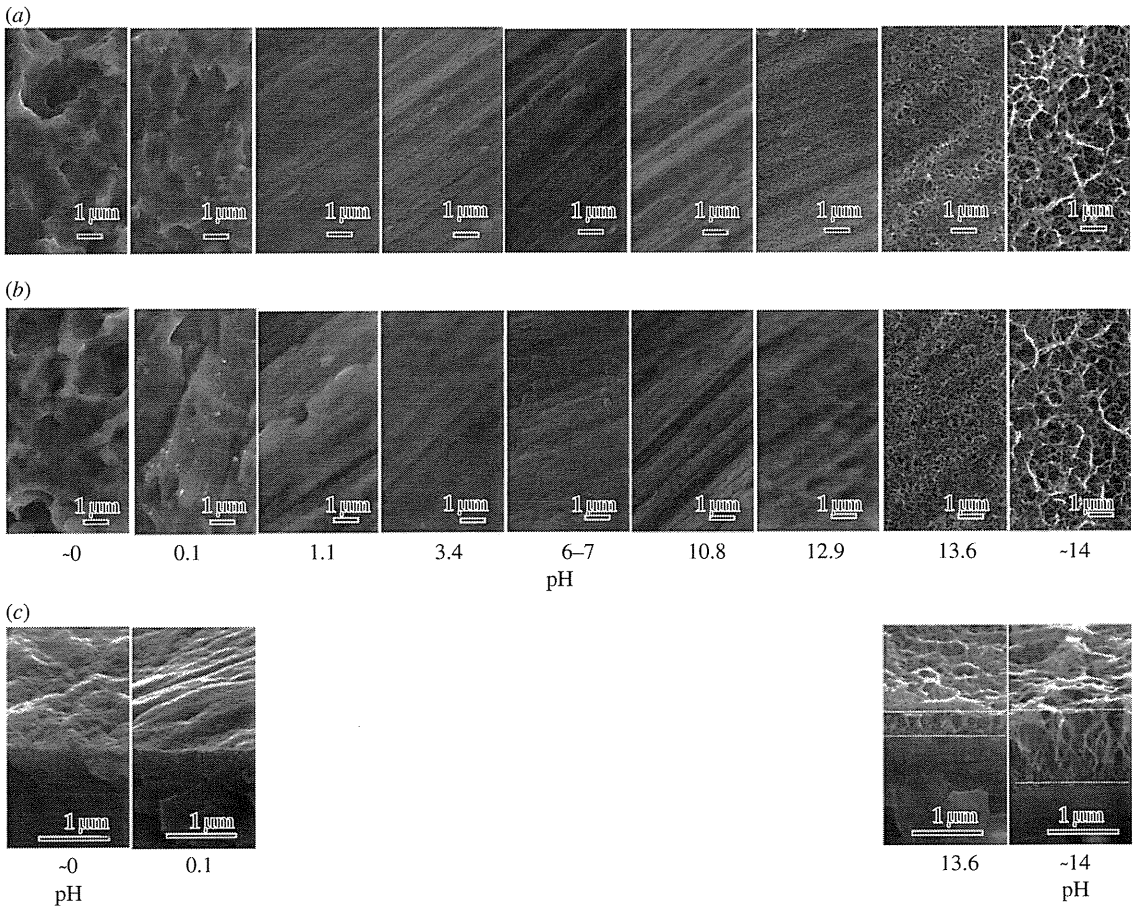

Figure 1. (*a*) Before and (*b*) after heat treatment. FE-SEM photographs of surfaces of Ti as exposed to solutions with different pHs, and those subsequently subjected to heat treatment. (*c*) Cross-sectional photographs of Ti metals exposed to solutions with low and high pHs and subsequently heat-treated are given at the bottom.

a pH lower than 0.1, while a nanometre scale roughness consisting of a network of feather-like phases that were elongated perpendicularly to the surface was formed on the Ti surface by exposure to solutions with a pH higher than 13.6. The Ti surface morphology was not changed by exposure to solutions with intermediate pHs ranging from 1.1 to 12.9. None of these topographies were essentially changed by the subsequent heat treatment.

Figure 2 shows TF-XRD patterns of the surfaces of the Ti specimens exposed to solutions with the different pHs, and also those that were subsequently heat-treated. It can be seen from figure 2 that titanium hydride (TH; TiH_x) [26] or sodium hydrogen titanate (SHT; $Na_xH_{2-x}Ti_3O_7$, $0 < x < 2$) [28] formed on the surface of Ti when treated with solutions of pH values lower than 0.1 or higher than 13.6, respectively. After the subsequent heat treatment, all the Ti specimens formed a titanium oxide of rutile phase irrespective of the pH of the solution. Only the pH values higher than 13.6 resulted in the formation of sodium titanate ($Na_2Ti_6O_{13}$) in addition to rutile after the heat treatment.

3.2. Zeta potential of the treated Ti metal

The zeta potential of a metal specimen with no electrically insulating oxide layer or one that was too thin cannot be measured by the present method, and hence the Ti specimens as exposed to the solutions could not be measured, because no or only a very thin oxide layer exists on their surfaces. This suggests that their zeta potentials are almost zero.

The zeta potentials of the Ti specimens subjected to the heat treatment after exposure to the solutions is shown in figure 3 as a function of the solution pH. Ti specimens exposed to solutions with a pH lower than 1.1 displayed a positive zeta potential higher than 5 mV, whereas those exposed to solutions with a pH higher than 13.6 displayed a negative zeta potential less than -10 mV. Those exposed to solutions with intermediate pH values that ranged from 3.4 to 12.9 had a zeta potential of approximately zero.

3.3. Distribution of elements near the surface

Figure 4 shows the depth profile of the GD-OES spectra of Ti specimens exposed to the solution with a pH $\sim$ 0 and also those that were subsequently subjected to heat treatment, as a function of sputtering time. Large amounts of H and O besides Ti were detected in the surface layer of the specimen exposed to the acid solution because of the formation of TH and titanium oxide by the acid treatment. It should be noted here that a small amount of Cl was also detected on its surface layer.

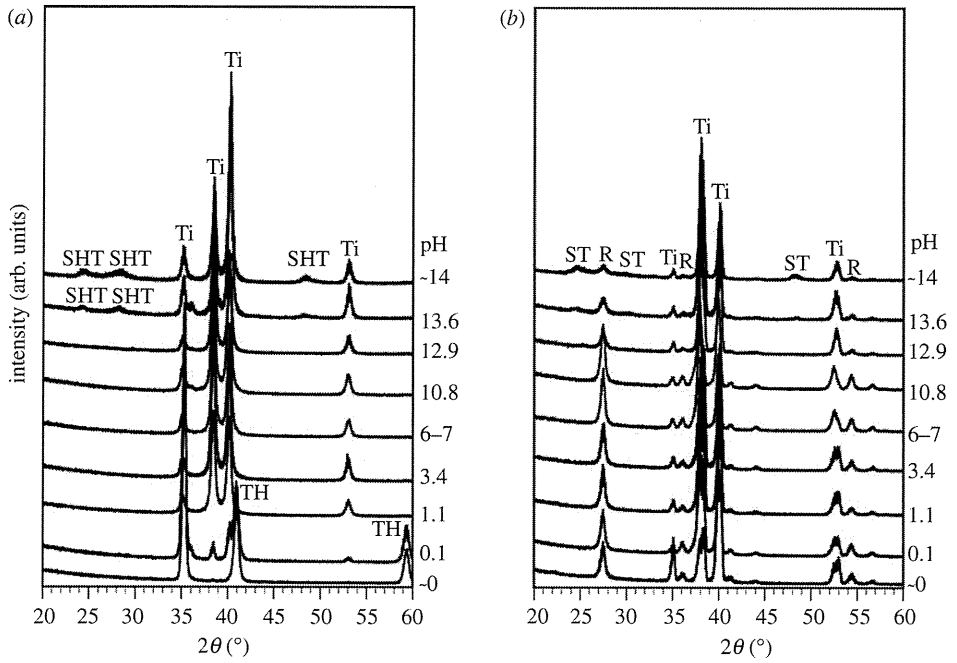

Figure 2. (*a*) Before and (*b*) after heat treatment. TF-XRD patterns of surfaces of Ti as exposed to solutions with different pHs, and those subsequently subjected to heat treatment. Ti, α Ti; TH, titanium hydride; SHT, sodium hydrogen titanate; ST, sodium titanate; R, rutile.

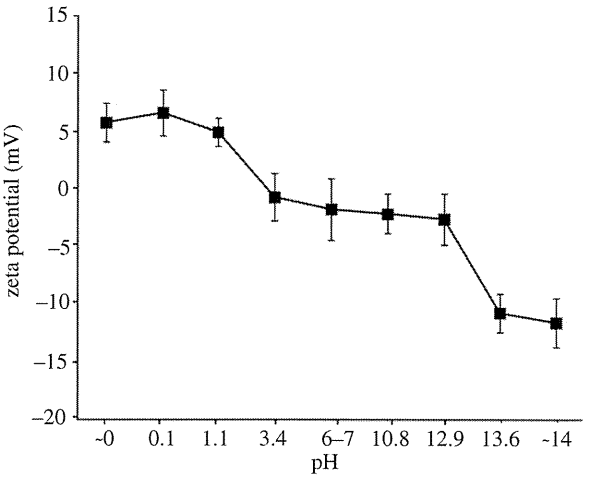

Figure 3. Zeta potentials of Ti as exposed to solutions with different pHs and subsequently subjected to heat treatment.

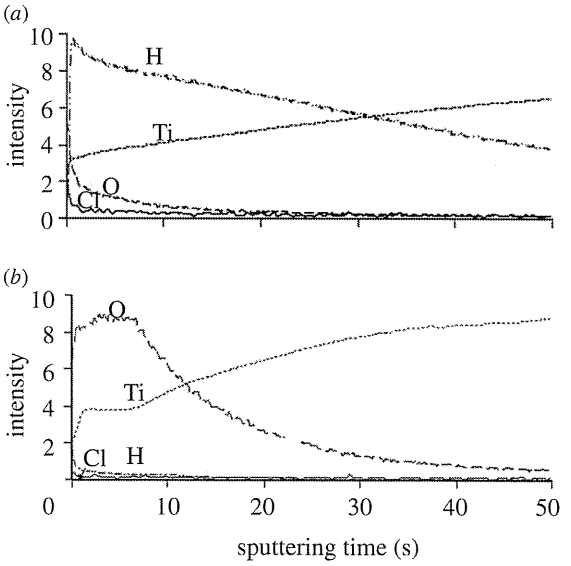

Figure 4. (*a*) Before and (*b*) after heat treatment. Depth profile of GD-OES spectra of surfaces of Ti as-exposed to the solutions with pH ~ 0 and that subsequently subjected to heat treatment, as a function of sputtering time.

The results show that H was remarkably reduced, while O was increased by the heat treatment because of transformation of the TH to titanium oxide. It should be noted here once again that a small amount of Cl was detected even after the heat treatment.

Depth profiles of elements near the surfaces of Ti specimens exposed to the NaOH solution with pH ~ 14 and those that were subsequently subjected to heat treatment were previously examined by Auger electron spectroscopy and already published [29]. According to the result, Na and O penetrated into the Ti specimen up to a depth of about 1 μm as a result of the NaOH treatment and their concentrations gradually decreased with increasing depth. Only O penetrated into a deeper region, while Na did not show any change in its distribution by the subsequent heat treatment.

3.4. Apatite-forming ability of treated Ti metal in simulated body fluid

The FE-SEM micrographs in figure 5 show the surface of the Ti specimens soaked in SBF for 3 days after

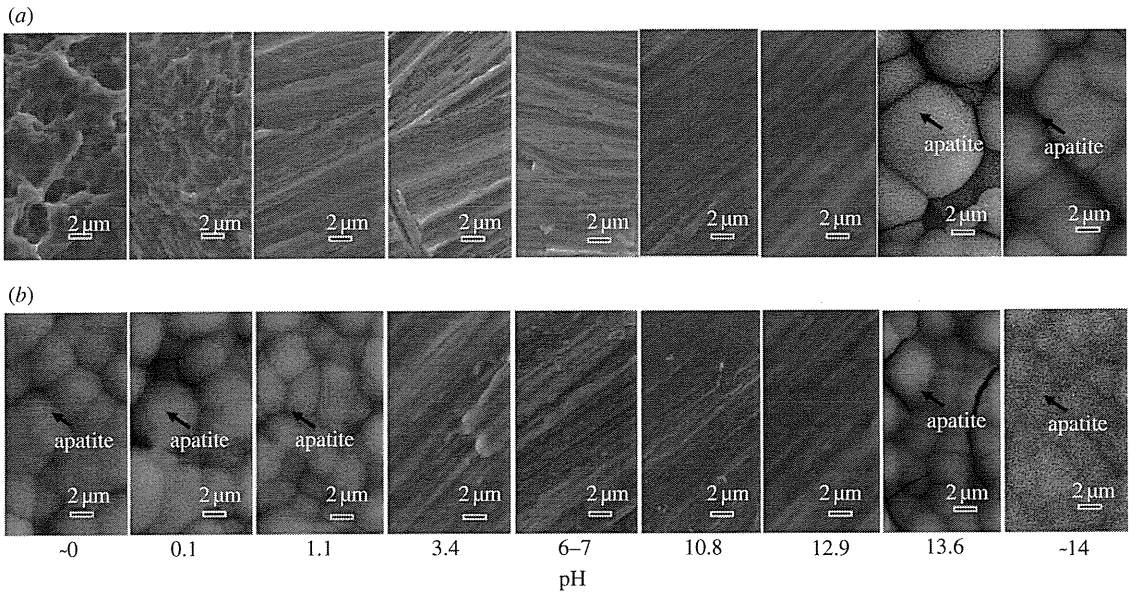

Figure 5. (*a*) Before and (*b*) after heat treatment. FE-SEM photographs of surfaces of Ti soaked in SBF for 3 days after exposure to solutions with different pHs, and those after subsequent heat treatment.

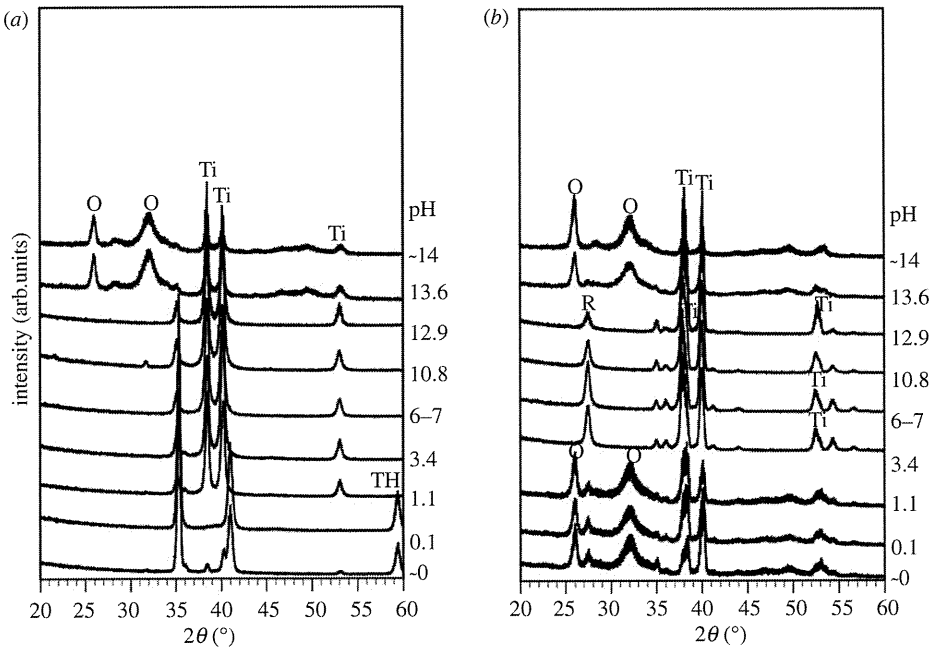

Figure 6. (*a*) Before and (*b*) after heat treatment. TF-XRD patterns of surfaces of Ti soaked in SBF for 3 days after exposure to solution with different pHs, and those after subsequent heat treatment, Ti, α Ti; TH, titanium hydride; R, rutile; O, apatite.

exposure to solutions with different pHs, and also those after the subsequent heat treatment. The TF-XRD patterns in figure 6 are of the surfaces of the Ti specimens soaked in SBF for 3 days after exposure to the solutions with the different pHs, and also those after the subsequent heat treatment. The spherical particles observed in the FE-SEM micrographs of the Ti surfaces were identified as crystalline apatite from the XRD patterns in figure 6. The Ti specimens as exposed to the solutions did not form the apatite on their surfaces except in the case of the solutions with pHs higher than 13.6, where only a relatively small amount of apatite was formed. In contrast, the Ti specimens after the heat treatment exhibited a large amount of apatite on their surfaces when they were exposed to solutions with a pH lower than 1.1 or higher than 13.6.

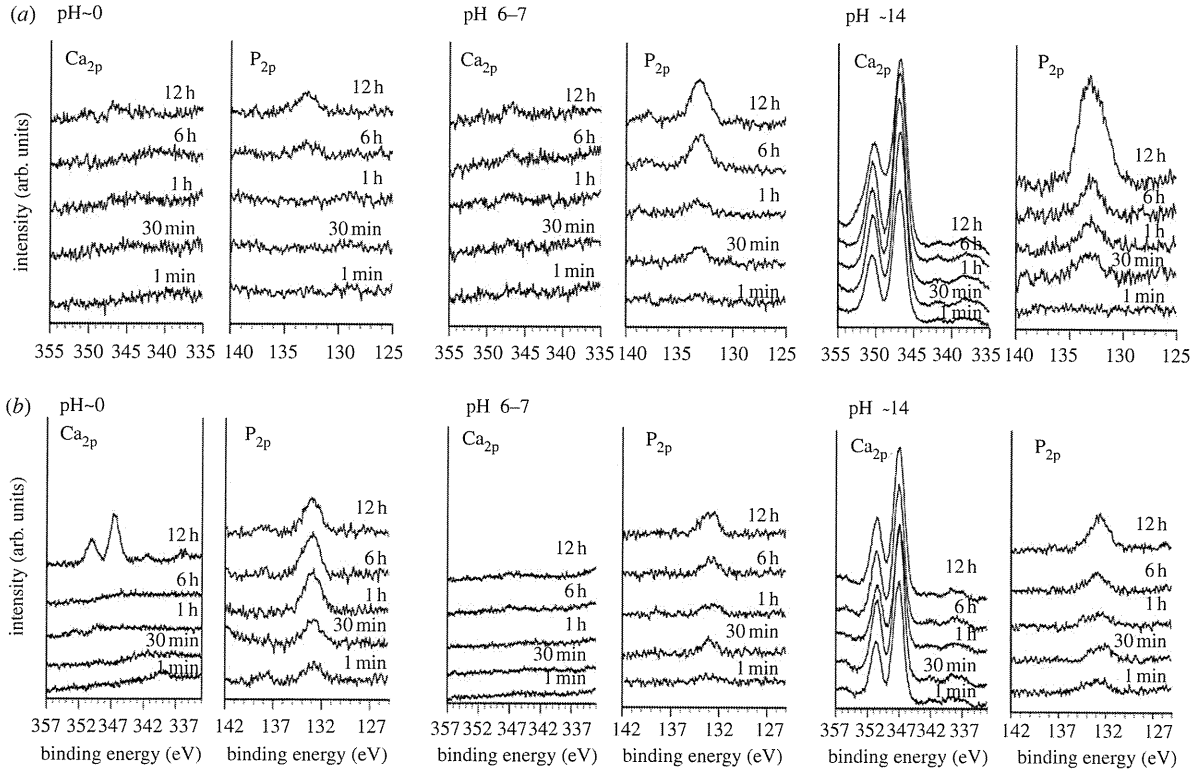

Figure 7. (*a*) XPS spectra of surfaces of Ti as exposed to solutions with pHs approximately 0, 6–7 and 14, and (*b*) those subsequent heat-treated as a function of soaking time in SBF.

Ti specimens exposed to solutions with an intermediate pH that ranged from 3.4 to 12.9 did not form any apatite, even after the heat treatment.

3.5. *X-ray photoelectron spectroscopy spectra of the treated Ti metal*

Figure 7 shows the Ca_{2P} and P_{2P} XPS spectra of the Ti surfaces exposed to solutions of pH values of approximately 0, 6–7 and 14 and those subsequently heat-treated as a function of soaking time in SBF. It can be seen that Ti specimens before heat treatment adsorb a small amount of the calcium and phosphate ions almost simultaneously, independent of pH, except in cases of a high pH, where it first selectively adsorbs the calcium ions, and then the phosphate ions.

In contrast, Ti specimens exposed to a low pH solution and subsequently heat-treated first selectively adsorb phosphate ions and then the calcium ions, whereas those exposed to a high pH and subsequently heat-treated do the opposite, i.e. first selectively adsorbing calcium ions and then phosphate ions. Ti specimens exposed to an intermediate pH adsorb a small amount of the calcium and phosphate ions almost simultaneously, even after the heat treatment.

4. DISCUSSION

It is apparent from figures 5 and 6 that the Ti specimens did not form surface apatite in SBF when exposed to the solutions, except when it was exposed to a strongly alkaline solution, which resulted in a small amount of apatite formation, whereas those that were subsequently heat-treated exhibited a large amount of apatite after exposure to strongly acidic or alkaline solutions.

Micrometre or nanometre scale roughness was produced on Ti specimens when they were exposed to strongly acidic or alkaline solutions, and this was not changed by the subsequent heat treatment, as shown in figure 1. This indicates that the surface morphology is not responsible for the increased apatite formation induced by the heat treatment. It should be emphasized that even the highly porous surface formed by the NaOH treatment was not responsible for apatite formation, because the highly porous surface was apparently not changed by the subsequent heat treatment, whereas the apatite formation was remarkably increased by the heat treatment, as shown by higher density of the apatite for heat-treated specimen on FE-SEM picture in figure 5.

TH or SHT was precipitated on Ti specimens when they were exposed to strongly acidic or alkaline solutions, and the precipitate was transformed into rutile or sodium titanate accompanied by rutile upon subsequent heat treatment (figure 2). This suggests that the rutile and sodium titanate are responsible for the increased apatite formation induced by the heat treatment. However, rutile was also detected on heat-treated Ti specimens after exposure to solutions with intermediate pH values (figure 2), which did not form the apatite. This indicates that the composition and structure of the rutile phase is not responsible for the increase in apatite formation induced by the heat treatment.

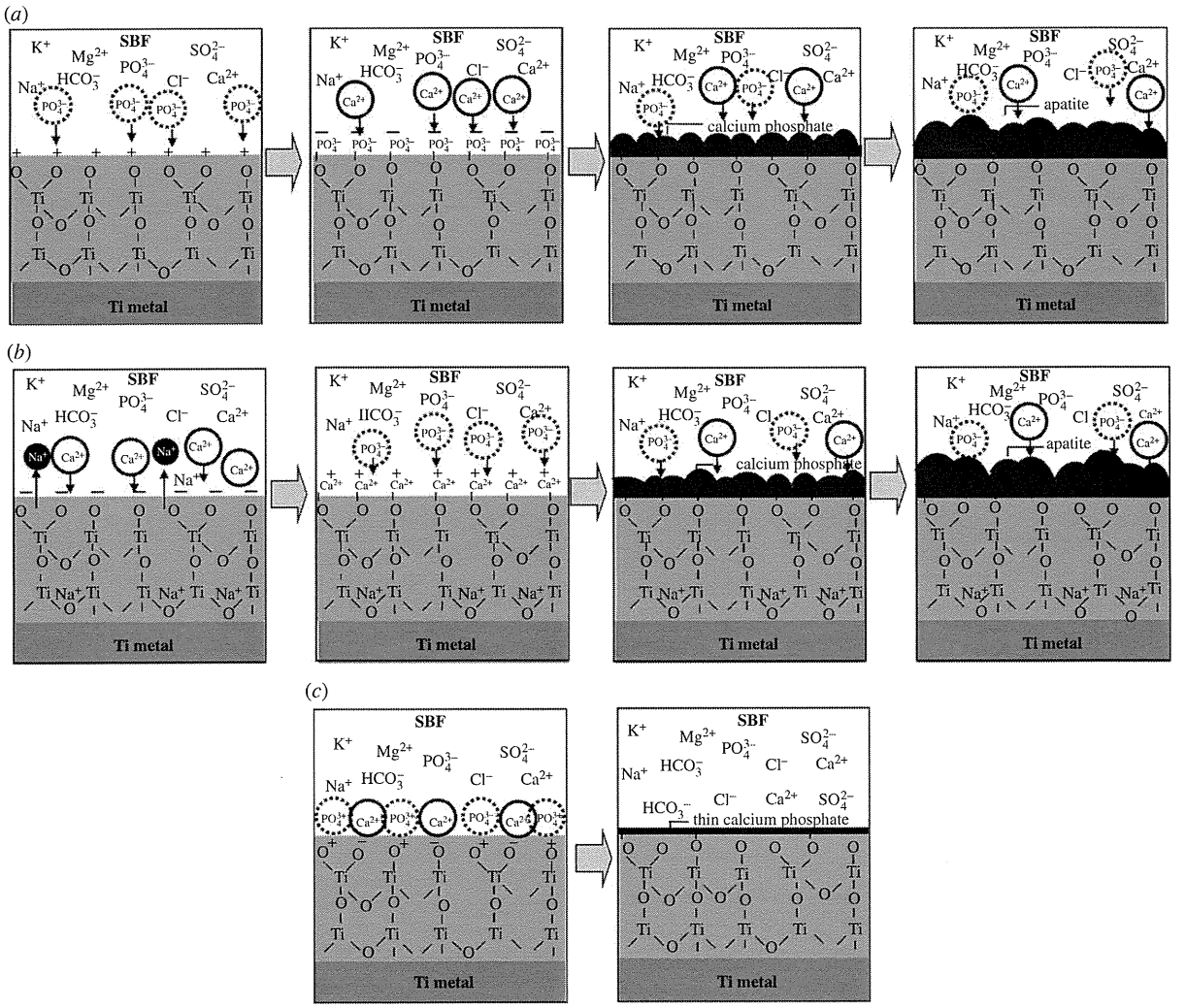

Figure 8. Schematic of ion adsorption on (*a*) positively charged, (*b*) negatively charged and (*c*) neutrally charged Ti metal.

The Ti specimens exposed to the solutions displayed a zeta potential of approximately zero, independent of the pH of the exposed solution, whereas those that were subsequently heat-treated displayed a certain level of positive or negative zeta potential when they were exposed to a strongly acidic or alkaline solution, respectively. This indicates that the certain level of the positive or negative surface charges is responsible for the apatite formation induced by the heat treatment. It is suggested that the positively charged surface first selectively adsorbs the negatively charged phosphate ions on its surface. As the phosphate ions accumulate, the surface becomes negatively charged. As a result, the positively charged calcium ions are adsorbed on its surface so as to produce a calcium phosphate which is eventually transformed into apatite, as shown in figure 8*a*. On the other hand, the negatively charged surface is assumed to first selectively adsorb positively charged calcium ions and then the negatively charged phosphate ions so as to also form apatite, as shown in figure 8*b*.

It is shown by the XPS spectra in figure 7 that the former type of phosphate and calcium ion adsorption occurred on heat-treated Ti specimens after exposure to strongly acidic solutions, while the latter type of sequential adsorption occurred on heat-treated Ti specimens after the strongly alkaline solutions.

The Ti specimen that was heat-treated after exposure to solutions with intermediate pH values exhibited a zeta potential of almost zero (figure 3). This means that the positively and negatively charged sites are balanced and hence the surface is neutrally charged [30]. It is assumed that each Ti site is able to simultaneously adsorb negatively charged phosphate ions and positively charged calcium ions, respectively, as shown in figure 8*c*. As a result, a thin calcium phosphate layer is formed on their surfaces and their charges are soon neutralized, and hence the calcium phosphate layer does not grow into the thick apatite layer in a short period of time. It is also evident from the XPS spectra in figure 7 that this type of simultaneous adsorption of the small amount of the phosphate and calcium ions occurred on Ti specimens that were heat-treated after exposure to solutions with intermediate pH value. However, the calcium phosphate layer was so thin that it was not apparently observed under FE-SEM with the

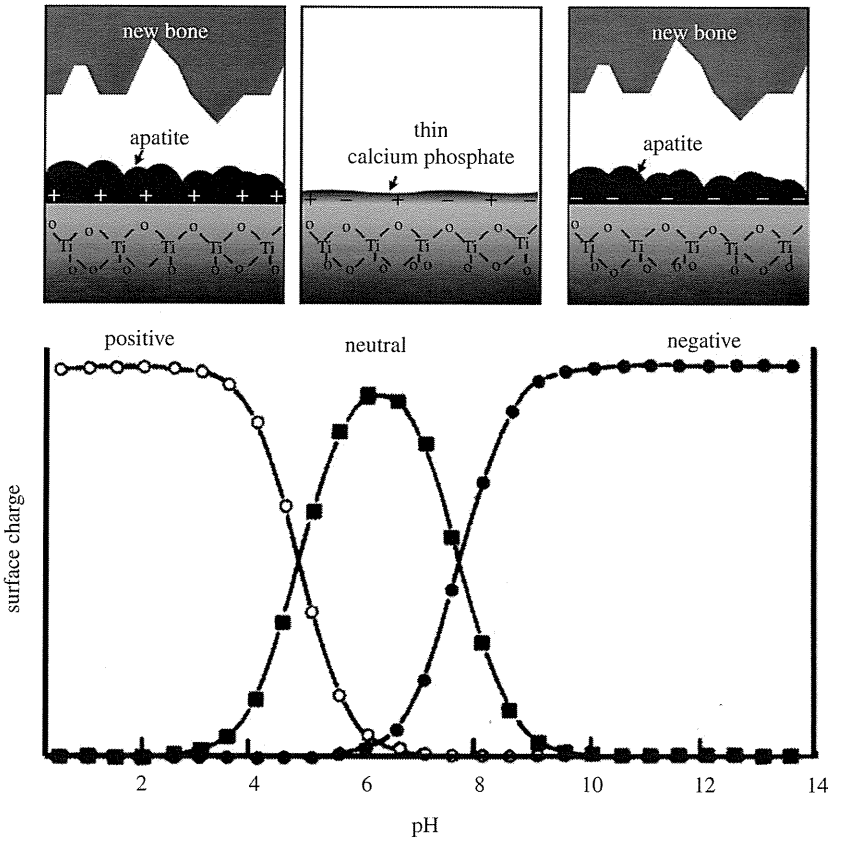

Figure 9. Apatite formation and bone-bonding of Ti as a function of pH of exposed solution. Lower part of this figure was reproduced from Textor *et al.* [30] after modification.

resolution of several nanometres in figure 5, and precipitation of apatite on the specimens was not detected by TF-XRD patterns in figure 6. The apatite formation on heat-treated Ti specimens after strong acid or alkali solutions is thus attributed to their positive or negative surface charges, respectively.

The reason why Ti specimens that are heat-treated after exposure to the strong acid solutions are charged positively may be due to the titanium oxide adsorbed with the Cl^- ions on their surfaces. It is assumed that the Cl^- ions were adsorbed on the TH on the surface of the Ti specimens when they were exposed to the strong acid solutions, and they remained on the titanium oxide that was formed on the Ti specimens by the subsequent heat treatment. The adsorption of the Cl^- ions on the TH on the Ti specimens exposed to the acid solutions and the adsorption of those on the titanium oxide on Ti specimens that were subsequently heat-treated were demonstrated by the GD-OES spectra shown in figure 4. These adsorbed Cl^- ions may become dissociated via exchange with OH^- ions in SBF so as to give rise to an acidic environment. It has been reported by Textor *et al.* [30] that titanium oxide is positively charged by forming larger numbers of $Ti\text{-}OH_2^+$ groups in acidic solutions. A recent report has shown that the positive charge and apatite formation on the Ti metal can be induced by not only Cl^-, but also other acid radicals such as NO_3^- and SO_4^{2-} [31].

The reason why Ti specimens that are heat-treated after exposure to strongly alkaline solutions are charged negatively may be due to the sodium titanate on their surfaces. The sodium titanate releases its Na^+ ions via exchange with the H_3O^+ ions in SBF to form Ti-OH groups on its surface [32–35] by the following reaction

$$\mathrm{Ti-ONa(metal)} + \mathrm{H_2O(SBF)} \rightarrow \mathrm{Ti-OH(metal)} + \mathrm{OH^-(SBF)} + \mathrm{Na^+(SBF)}$$

This increases the pH of the surrounding SBF because of the consumption of H_3O^+ ions. It has been reported by Textor *et al.* [30] that titanium oxide is negatively charged by forming $Ti\text{-}O^-$ groups in alkaline solution.

In the case of the Ti specimens prior to heat treatment, they became covered with a thin titanium oxide layer when they were exposed to the solutions with intermediate pH values, similar to the untreated Ti specimen. This titanium oxide layer has an almost neutral surface charge (figure 3) and hence does not induce the apatite formation. They did form TH on their surfaces when they were exposed to the strongly acidic solutions. This phase is electrically conductive [36]. Therefore, their surfaces are hardly charged even though they adsorbed Cl^- ions, and hence did not induce the apatite formation.

Ti specimens formed an SHT on their surfaces upon exposure to strongly alkaline solutions. The SHT also releases its Na^+ ions via exchange with H_3O^+ ions in

SBF to form negatively charged Ti-OH groups [37]. However, SHT is electrically conductive, and hence its negative surface charge is so small that it cannot be measured by the present method. Therefore, Ti specimens exposed to the strongly alkaline solution induced apatite formation, but its magnitude was smaller than that of the Ti specimen that was subsequently heat-treated, as shown in figure 5. It is apparent from these findings that the Ti specimen that is heat-treated after exposure to a strongly acidic or alkaline solution can induce surface apatite formation in SBF, because of its large positive or negative surface charges.

It has been shown for various kinds of ceramics, including glasses, glass-ceramics and sintered crystalline ceramics of various compositions, that materials that have the capacity to form a surface apatite layer in the living body are able to bond to living bone through the apatite layer [27], and are useful as long as they contain neither cytotoxic nor antigenic components, and furthermore, their apatite formation can be reproduced even in an acellular SBF having ion concentrations almost equal to those of human blood plasma [27]. Bohner *et al.* [38] and Pan *et al.* [39] recently pointed out that certain resorbable ceramics bond to living bone without any formation of a surface apatite layer. These exceptional cases were also pointed out in the paper described earlier [27]. This means that the rule described earlier should be applied with caution in the case of resorbable materials. However, Ti is not a resorbable material, and contains neither cytotoxic nor antigenic components. It has already been shown that Ti and various kinds of Ti-based alloys (such as Ti–6Al–4V, Ti–15Mo–5Zr–3Al and Ti–15Zr–4Nb–4Ta) that are able to form apatite on their surfaces in SBF, bond to living bone through the apatite layer formed on their surfaces in the living body [23,24,26,40–47].

In view of these findings, it is predicted from the present results that Ti forms a bone-like apatite surface layer in the living body and bonds to living bone through the apatite layer upon exposure to a strongly acidic or alkaline solution and then heat-treated, because its surface is then either positively or negatively charged in the living body. In contrast with this, Ti exposed to solutions with intermediate pH values and subsequently subjected to the heat treatment forms only a thin amorphous calcium phosphate layer in the living body, and hence possesses a good compatibility with the bone but does not bond to bone, because the surface is almost neutrally charged, as shown in figure 9. The Ti not subjected to heat treatment after the solution treatment displayed little or no surface apatite formation in the living body, and hence do not bond to living bone, because their surfaces are almost entirely neutrally charged.

5. CONCLUSION

Ti specimens that were heat-treated after exposure to strong acid or alkali solutions showed remarkable apatite formation on their surfaces in SBF, while those heat-treated after exposure to solutions with intermediate pHs did not show any such apatite formation.

The remarkable apatite formation of Ti exposed to the strongly acidic and alkaline solutions is attributed to the magnitude of their positive and negative surface charges, respectively. The positive and negative surface charges are produced by the dissociated chloride ions and the released sodium ions, respectively. The lack of apatite formation on the Ti exposed to intermediate pH solutions is attributed to their neutral surface charges. Ti that were not subjected to heat treatment after the solutions showed no or only a little apatite formation on their surfaces in SBF because of their neutral surface charge.

It is predicted from the present results that the bone-bonding property of Ti strongly depends upon the pH of the solution used, i.e. Ti forms bone-like apatite on its surface in the living body and bonds to living bone through the apatite layer, if it is heat-treated after exposure to a strongly acidic or alkaline solution.

REFERENCES

1 Brunette, D. M., Tengvall, P., Textor, M. & Thomsen, P. 2001 *Titanium in medicine*. Berlin, Germany: Springer.

2 Yan, W. Q., Nakamura, T., Kobayashi, M., Kim, H. M., Miyaji, F. & Kokubo, T. 1997 Bonding of chemically treated titanium implants to bone. *J. Biomed. Mater. Res.* **37**, 267–275. (doi:10.1002/(SICI)1097-4636(199711)37:2, 267::AID-JBM17.3.0.CO;2-B)

3 Hanawa, T., Kaminura, Y., Yamamoto, S., Kohgo, T., Amemiya, A., Ukai, M., Murakami, K. & Asaoka, K. 1997 Early bone formation around calcium-ion-implanted titanium inserted into rat tibia. *J. Biomed. Mater. Res.* **36**, 131–136. (doi:10.1002/(SICI)1097-4636(199707)36: 1<131::AID-JBM16>3.0.CO;2-L)

4 Armitage, D. A., Mihoc, R., Tate, T. J., McPhail, D. S., Chater, R., Hobkirk, J. A., Shinawi, L. & Jones, F. H. 2007 The oxidation of calcium implanted titanium in water: a depth profiling study. *Appl. Surf. Sci.* **253**, 4085–4093. (doi:10.1016/j.apsusc.2006.09.006)

5 Nayab, H., Jones, F. H. & Olsen, I. 2007 Effects of calcium ion-implantation of titanium on bone cell function *in vitro*. *J. Biomed. Mater. Res.* **83A**, 296–302. (doi:10.1002/jbm.a.31218)

6 Sul, Y. T. 2003 The significance of the surface properties of oxidized titanium to the bone response: special emphasis on potential biochemical bonding of oxidized titanium implant. *Biomaterials* **24**, 3893–3907. (doi:10.1016/S0142-9612(03)00261-8)

7 Song, W. H., Ryu, H. S. & Hong, S. H. 2005 Apatite induction on Ca-containing titania formed by micro-arc oxidation. *J. Am. Ceram. Soc.* **88**, 2642–2644. (doi:10.1111/j.1551-2916.2005.00476.x)

8 Frojd, V., Franke-Stenport, V., Meirelles, L. & Wennerberg, A. 2008 Increased bone contact to a calcium-incorporated oxidized commercially pure titanium implant: an *in-vivo* study in rabbits. *Int. J. Oral Maxillofac. Surg.* **37**, 561–566. (doi:10.1016/j.ijom.2008.01.020)

9 Wu, J., Liu, Z. M., Zhao, X. H., Gao, Y., Hu, J. & Gao, B. 2010 Improved biological performance of microarc-oxidized low-modulus Ti-24Nb-4Zr-7.9Sn alloy. *J. Biomed. Mater. Res.* **92B**, 298–306. (doi:10.1002/jbm.b.31515)

10 Whiteside, P., Matykina, E., Gough, J. F., Skeldon, P. & Thompson, G. E. 2010 *In vitro* evaluation of cell proliferation and collagen synthesis on titanium following plasma electrolytic oxidation. *J. Biomed. Mater. Res.* **94A**, 38–46. (doi:10.1002/jbm.a.32664)

11 Nakagawa, M., Zhang, L., Udoh, K., Matsuya, S. & Ishikawa, K. 2005 Effects of hydrothermal treatment with $CaCl_2$ solution on surface property and cell response of titanium implants. *J. Mater. Sci., Mater. Med.* **16**, 985–991. (doi:10.1007/s10856-005-4753-0)

12 Park, J. W., Park, K. B. & Suh, J. Y. 2007 Effects of calcium ion incorporation on bone healing of Ti6Al4V alloy implants in rabbit tibiae. *Biomaterials* **28**, 3306–3313. (doi:10.1016/j.biomaterials.2007.04.007)

13 Ueda, M., Ikeda, M. & Ogawa, M. 2009 Chemical–hydrothermal combined surface modification of titanium for improvement of osteointegration. *J. Mater. Sci. Eng. C* **29**, 994–1000. (doi:10.1016/j.msec.2008.09.002)

14 Chen, X. B., Li, Y. C., Plessis, J. D., Hodgson, P. D. & Wen, C. 2009 Influence of calcium ion deposition on apatite-inducing ability of porous titanium for biomedical applications. *Acta Biomater.* **5**, 1808–1820. (doi:10.1016/j.actbio.2009.01.015)

15 Park, J. W., Kim, Y. J., Jang, J. H., Kwon, T. G., Bae, Y. C. & Suh, J. Y. 2010 Effects of phosphoric acid treatment of titanium surfaces on surface properties, osteoblast response and removal of torque forces. *Acta Biomater.* **6**, 1661–1670. (doi:10.1016/j.actbio.2009.10.011)

16 Wang, X. X., Hayakawa, S., Tsuru, K. & Osaka, A. 2002 Bioactive titania gel layers formed by chemical treatment of Ti substrate with a H_2O_2/HCl solution. *Biomaterials* **23**, 1353–1357. (doi:10.1016/S0142-9612(01)00254-X)

17 Wang, X. X., Yan, W., Hayakawa, S., Tsuru, K. & Osaka, A. 2003 Apatite deposition on thermally and anodically oxidized titanium surfaces in a simulated body fluid. *Biomaterials* **24**, 4631–4637. (doi:10.1016/S0142-9612(03)00357-0)

18 Wu, J. M., Hayakawa, S., Tsuru, K. & Osaka, A. 2004 Low temperature preparation of anatase and rutile layers on titanium substrates and their ability to induce *in vitro* apatite deposition. *J. Am. Ceram. Soc.* **87**, 1635–1642. (doi:10.1111/j.1551-2916.2004.01635.x)

19 Lu, X., Wang, Y., Yang, X., Zhang, Q., Zhao, Z., Weng, L. T. & Leng, Y. 2008 Spectroscopic analysis of titanium surface functional groups under various surface modification and their behaviors *in vitro* and *in vivo*. *J. Biomed. Mater. Res.* **84A**, 523–534. (doi:10.1002/jbm.a.31471)

20 Sugino, A., Ohtsuki, C., Tsuru, K., Hayakawa, S., Nakano, T., Okazaki, Y. & Osaka, A. 2009 Effect of spatial design and thermal oxidation on apatite formation on Ti–15Zr–4Ta–4Nb alloy. *Acta Biomater.* **5**, 298–304. (doi:10.1016/j.actbio.2008.07.014.)

21 Karthega, M. & Rajendran, N. 2010 Hydrogen peroxide treatment on Ti–6Al–4V alloy: a promising surface modification technique for orthopaedic application. *Appl. Surf. Sci.* **256**, 2176–2183. (doi:10.1016/j.apsusc.2009.09.069)

22 Kokubo, T., Miyaji, F., Kim, H. M. & Nakamura, T. 1996 Spontaneous formation of bonelike apatite layer on chemically treated titanium metals. *J. Am. Ceram. Soc.* **79**, 1127–1129. (doi:10.1111/j.1151-2916.1996.tb08561.x)

23 Kim, H. M., Miyaji, F., Kokubo, T. & Nakamura, T. 1996 Preparation of bioactive Ti and its alloy via simple chemical surface treatment. *J. Biomed. Mater. Res.* **32**, 409–417. (doi:10.1002/(SICI)1097-4636(199611)32:3<409:: AID-JBM14>3.0.CO;2-B)

24 Nishiguchi, S., Fujibayashi, S., Kim, H. M., Kokubo, T. & Nakamura, T. 2003 Biology of alkali- and heat-treated titanium implants. *J. Biomed. Mater. Res.* **67A**, 26–35. (doi:10.1002/jbm.a.10540)

25 Kawanabe, K., Ise, K., Goto, K., Akiyama, H., Nakamura, T., Kaneuji, A., Sugimori, T. & Matsumoto, T. 2009 A new cementless total hip arthoplasty with bioactive titanium porous-coating by alkaline and heat treatment: average 4.8-year results. *J. Biomed. Mater. Res.* **90B**, 476–481. (doi:10.1002/jbm.b.31309)

26 Kokubo, T., Pattanayak, D. K., Yamaguchi, S., Takadama, H., Matsushita, T., Kawai, T., Takemoto, M., Fujibayashi, S. & Nakamura, T. 2010 Positively charged bioactive Ti metal prepared by simple chemical and heat treatments. *J. R. Soc. Interface* **7**, S503–S513. (doi:10.1098/rsif.2010.0129.focus)

27 Kokubo, T. & Takadama, H. 2006 How useful is SBF in predicting *in vivo* bone bioactivity? *Biomaterials* **27**, 2907–2915. (doi:10.1016/j.biomaterials.2006.01.017)

28 Sun, X. & Li, Y. 2003 Synthesis and characterization of ion-exchangeable titanate nanotubes. *Chem. Eur. J.* **9**, 2229–2238. (doi:10.1002/chem.200204394)

29 Kim, H.-M., Miyaji, F., Kokubo, T., Nishiguchi, S. & Nakamura, T. 1999 Graded surface structure of bioactive titanium prepared by chemical treatment. *J. Biomed. Mater. Res.* **45**, 100–107. (doi:10.1002/(SICI)1097-4636(199905)45:2<100::AID-JBM4>3.0.CO;2-0)

30 Textor, M., Sittig, C., Frauchiger, V., Tosatti, S. & Brunette, D. M. 2001 Properties and biological significance of natural oxide films on titanium and its alloys. In *Titanium in medicine* (eds D. M. Brunette, P. Tengvall, M. Textor & P. Thomsen), pp. 171–230. Berlin, Germany: Springer.

31 Pattanayak, D. K., Yamaguchi, S., Matsushita, T. & Kokubo, T. 2011 Nanostructured positively charged bioactive TiO_2 layer formed on Ti metal by NaOH, acid and heat treatments. *J. Mater. Sci: Mater. Med.* **22**, 1803–1812. (doi:10.1007/s10856-011-4372-x)

32 Kawai, T., Kizuki, T., Takadama, T., Matsushita, T., Unuma, H., Nakamura, T. & Kokubo, T. 2010 Apatite formation on surface titanate layer with different Na content on Ti metal. *J. Ceram. Soc. Japan* **118**, 19–24.

33 Takadama, H., Kim, H.-M., Kokubo, T. & Nakamura, T. 2001 An X-ray photoelectron spectroscopy study of the process of apatite formation on bioactive titanium metal. *J. Biomed. Mater. Res.* **55**, 185–193. (doi:10.1002/1097-4636(200105)55:2<185::AID-JBM1005>3.0.CO;2-P)

34 Takadama, H., Kim, H.-M., Kokubo, T. & Nakamura, T. 2001 TEM-EDX study of mechanism of bonelike apatite formation on bioactive titanium metal in simulated body fluid. *J. Biomed. Mater. Res.* **57**, 441–448. (doi:10.1002/1097-4636(20011205)57:3<441::AID-JBM1187>3.0.CO;2-B)

35 Kim, H. M., Himeno, T., Kawashita, M., Lee, J. H., Kokubo, T. & Nakamura, T. 2003 Surface potential change in bioactive titanium metal during the process of apatite formation in simulated body fluid. *J. Biomed. Mater. Res. A* **67**, 1305–1309. (doi:10.1002/jbm.a.20039)

36 Ito, M., Setoyama, D., Matsunaga, J., Muta, H., Kurosaki, K., Masayoshi, U. & Yamanaka, S. 2006 Electrical and thermal properties of titanium hydrides. *J. Alloys Compd.* **420**, 25–28. (doi:10.1016/j.jallcom.2005.10.032)

37 Kim, H.-M., Miyaji, F., Kokubo, T. & Nakamura, T. 1997 Apatite-forming ability of alkali-treated Ti metal in body environment. *J. Ceram. Soc. Japan* **105**, 111–116.

38 Bohner, M. & Lemahitre, J. 2009 Can bioactivity be tested *in vitro* with SBF solution? *Biomaterials* **30**, 2175–2179. (doi:10.1016/j.biomaterials.2009.01.008)

39 Pan, H., Zhao, X., Darvell, B. W. & Lu, W. W. 2010 Apatite-formation ability: predictor of 'bioactivity'? *Acta Biomater.* **6**, 4181–4188. (doi:10.1016/j.actbio.2010.05.013)

40 Nishiguchi, S., Kato, H., Fujita, H., Kim, H. M., Miyaji, F., Kokubo, T. & Nakamura, T. 1999 Enhancement of bone-bonding strengths of titanium alloy implants by alkali and heat treatments. *J. Biomed. Mater. Res.* (*Appl Biomater.*) **48**, 689–696. (doi:10.1002/(SICI)1097-4636(1999)48:5<689::AID-JBM13>3.0.CO;2-C)

41 Kim, H. M., Takadama, H., Miyaji, F., Kokubo, T., Nishiguchi, S. & Nakamura, T. 2000 Formation of bioactive functionally graded structure on Ti–6Al–4V alloy by chemical surface treatment. *J. Mater. Sci., Mater. Med.* **11**, 555–559. (doi:10.1023/A:1008924102096)

42 Kim, H. M., Takadama, H., Kokubo, T., Nishiguchi, S. & Nakamura, T. 2000 Formation of a bioactive graded surface structure on Ti–15Mo–5Zr–3Al alloy by chemical treatments. *Biomaterials* **21**, 353–358. (doi:10.1016/S0142-9612(99)00190-8)

43 Takemoto, M., Fujibayashi, S., Neo, M., So, K., Akiyama, N., Matsushita, T., Kokubo, T. & Nakamura, T. 2007 A porous bioactive titanium implant for spinal interbody fusion: an experimental study using a canine model. *J. Neurosurg. Spine* **7**, 435–443. (doi:10.3171/SPI-07/10/435)

44 Yamaguchi, S., Takadama, H., Matsushita, T., Nakamura, T. & Kokubo, T. 2010 Apatite-forming ability of Ti–15Zr–4Nb–4Ta alloy induced by calcium solution treatment. *J. Mater. Sci., Mater. Med.* **21**, 439–444. (doi:10.1007/s10856-009-3904-0)

45 Kizuki, T., Takadama, H., Matsushita, T., Nakamura, T. & Kokubo, T. 2010 Preparation of bioactive Ti metal surface enriched with calcium ions by chemical treatment. *Acta Biomater.* **6**, 2836–2842. (doi:10.1016/j.actbio.2010.01.007)

46 Fukuda, A. *et al.* 2011 Bone bonding bioactivity of Ti metal and Ti–Zr–Nb–Ta alloys with Ca ions incorporated on their surfaces by simple chemical and heat treatment. *Acta Biomater.* **7**, 1379–1386. (doi:10.1016/j.actbio.2010.09.026)

47 Pattanayak, D. K., Fukuda, A., Matsushita, T., Takemoto, M., Fujibayashi, S., Sasaki, K., Nishida, N., Nakamura, T. & Kokubo, T. 2011 Bioactive Ti metal analogous to human cancellous bone: fabrication by selective laser melting and chemical treatments. *Acta Biomater.* **7**, 1398–1406. (doi:10.1016/j.actbio.2010.09.034)

Acta Biomaterialia 7 (2011) 1398–1406

Contents lists available at ScienceDirect

Acta Biomaterialia

journal homepage: www.elsevier.com/locate/actabiomat

Bioactive Ti metal analogous to human cancellous bone: Fabrication by selective laser melting and chemical treatments

Deepak K. Pattanayak [a,*,1], A. Fukuda [b,1], T. Matsushita [a], M. Takemoto [b], S. Fujibayashi [b], K. Sasaki [c], N. Nishida [c], T. Nakamura [b], T. Kokubo [a]

[a] Department of Biomedical Sciences, College of Life and Health Sciences, Chubu University, Japan
[b] Department of Orthopaedic Surgery, Graduate School of Medicine, Kyoto University, Japan
[c] Sagawa Printing Co. Ltd., Kyoto, Japan

ARTICLE INFO

Article history:
Received 10 August 2010
Received in revised form 22 September 2010
Accepted 24 September 2010
Available online 29 September 2010

Keywords:
Selective laser melting
Porous titanium
Chemical treatment
Compressive strength
In vitro and in vivo studies

ABSTRACT

Selective laser melting (SLM) is a useful technique for preparing three-dimensional porous bodies with complicated internal structures directly from titanium (Ti) powders without any intermediate processing steps, with the products being expected to be useful as a bone substitute. In this study the necessary SLM processing conditions to obtain a dense product, such as the laser power, scanning speed, and hatching pattern, were investigated using a Ti powder of less than 45 μm particle size. The results show that a fully dense plate thinner than 1.8 mm was obtained when the laser power to scanning speed ratio was greater than 0.5 and the hatch spacing was less than the laser diameter, with a 30 μm thick powder layer. Porous Ti metals with structures analogous to human cancellous bone were fabricated and the compressive strength measured. The compressive strength was in the range 35–120 MPa when the porosity was in the range 75–55%. Porous Ti metals fabricated by SLM were heat-treated at 1300 °C for 1 h in an argon gas atmosphere to smooth the surface. Such prepared specimens were subjected to NaOH, HCl, and heat treatment to provide bioactivity. Field emission scanning electron micrographs showed that fine networks of titanium oxide were formed over the whole surface of the porous body. These treated porous bodies formed bone-like apatite on their surfaces in a simulated body fluid within 3 days. In vivo studies showed that new bone penetrated into the pores and directly bonded to the walls within 12 weeks after implantation into the femur of Japanese white rabbits. The percentage bone affinity indices of the chemical- and heat-treated porous bodies were significantly higher than that of untreated implants.

1. Introduction

Titanium (Ti) metal and its alloys are widely used for various implants in the orthopedic and dental fields, because of their good biocompatibility and high mechanical strength. However, their elastic moduli are higher than that of living bone and, hence, they are liable to induce bone resorption due to stress shielding. If a considerable amount of interconnected pores are introduced into them, their elastic moduli decrease to the level of cancellous bone. In addition, bone tissue can grow into the pores to integrate with them. Therefore, various methods have been developed for producing porous bodies of Ti metal and its alloys [1]. Among them, the most common method is sintering of metal powders with added volatile materials [2,3]. Recently, selective laser sintering (SLS) [4–10], selective laser melting (SLM) or direct laser forming (DLF) [11–18] and selective electron beam melting (SEBM) [19] processes have been applied to produce porous bone substitutes. The SLS process produces a porous body by partial sintering of metal powders. On the other hand, in the DLF/SLM and SEBM processes the metal powders are completely melted and fused by a laser or electron beam, respectively, resulting in a porous body within a short period of time [13,19]. Attempts have been made to produce various kinds of porous Ti metal with simple interconnected porous structures by the SLM process [11,12,17]. However, preparation of porous Ti metal with a structure analogous to human cancellous bone has not been reported.

In the SLM process three-dimensional (3D) structures can be prepared from metal powders without any additional processing steps. However, in order to obtain a defect-free specimen, it is essential to optimize the processing parameters of the SLM technique, i.e. laser power, scanning speed, hatching pattern, etc.

Although Ti metal and titanium alloys are biocompatible, they do not bond to living bone directly when implanted into a bone defect [20]. However, Ti metal subjected to NaOH and heat treatments to form sodium titanate on its surface spontaneously bonds

* Corresponding author. Tel.: +81 568 51 9731; fax: +81 568 51 5370.
E-mail addresses: deepak@isc.chubu.ac.jp, deepak_pattanayak@rediffmail.com (D.K. Pattanayak).
[1] The first two authors contributed equally to this study.

1742-7061/$ - see front matter © 2010 Acta Materialia Inc. Published by Elsevier Ltd. All rights reserved.
doi:10.1016/j.actbio.2010.09.034

Table 1
Chemical composition of the titanium powder (mass%).

O	Fe	H	C	N	Ni	Cr	Si	Ti
0.121	0.029	0.005	0.010	0.006	0.003	0.003	0.001	Balance

to living bone through an apatite layer formed on its surface in the living body [21–23]. This bioactive Ti metal has been applied to an artificial hip joint, and its effectiveness has already been confirmed in clinical trials [24]. This bioactive artificial hip joint (AHFIX, Japan Medical Materials Co., Japan) has been approved for clinical use in Japan since 2007.

Ti metal subjected to NaOH, HCl, and heat treatments to form Na-free titanium oxide on its surface has also been found to form a bone-like apatite layer in a simulated body fluid (SBF) [25] and to exhibit osteoconductivity as well as osteoinductivity [26–28].

In the present study plate specimens were first fabricated by the SLM process using commercially pure Ti powders. The effect of processing parameters such as power, scanning speed, and scanning pattern of the laser beam on the density of the plate specimens was investigated. Porous Ti metal with a structure analogous to human cancellous bone was prepared using the optimum operating conditions and its compressive strength measured. It was subjected to NaOH, HCl, and heat treatment for bioactivation and its apatite-forming ability in SBF and bone-bonding abilities in rabbit femurs examined.

2. Materials and methods

2.1. Materials

A gas atomized commercially pure Ti metal powder (grade 2, Osaka Titanium Technologies Co. Ltd., Japan) with a particle size of <45 μm was used as the starting powder. Its chemical composition is given in Table 1.

2.2. Selective laser melting

2.2.1. Determination of optimum conditions

Fig. 1 shows schematically the selective laser melting process. In the present experiment an SLM system (EOSINT-M270, Electro Optical Systems GmbH, Germany) was used. A 3D model was designed by computer-aided design (CAD) software (Magics, Materialise, Belgium). This 3D model was horizontally sliced into many thin layers of two-dimensional images. In this system a Yb fiber laser beam of nominal diameter 100 μm and with a maximum power of 200 W moves at a maximum speed of 7000 mm s^{-1} in an argon gas environment. According to the data for the slices provided by the computer the laser beam scans the Ti metal powder layer to selectively melt it, producing the prescribed two-dimensional metallic structures. In the next step the platform moves vertically downwards, allowing the deposition of an unfused powder layer at a 30 μm interval. Again, the laser beam selectively melts the second layer over the first layer, and this process is continued repeatedly to construct the final 3D metallic structure. The manufactured specimen was removed from the platform. The specimens were cleaned ultrasonically using acetone, 2-propanol, and ultrapure water for 30 min each to remove residual unfused powder sticking to the walls of the specimen.

Fig. 2 shows the standard scanning strategy for the fabrication of the specimen using a boundary contour beam of 58.5 W power followed by a hatch beam of 117 W, with a hatch space of 180 μm and a hatch offset of 20 μm. In each subsequent layer the hatch lines are rotated with respect to the previous layer by 66.7° to melt the powder completely. In order to investigate the effect of energy density on the density of the fabricated specimen, the laser power was varied from 90 to 180 W at a constant scanning speed of 225 mm s^{-1} and constant powder layer of 30 μm thickness, so that the power to speed ratio (P/V) was in the range 0.3–0.8 W mm^{-1} s^{-1}. Specimens of $9 \times 9 \times 9$ mm^3 size were formed at different P/V ratios. Their densities were measured using Archimedes' principle. In addition to the above, $9 \times 9 \times t$ mm^3 specimens of different thicknesses (t) were formed by using a hatch space of 90 and 180 μm, and their densities were also measured using the same technique.

2.2.2. Fabrication of a porous structure analogous to human cancellous bone

Porous Ti metals with a structure similar to that of human cancellous bone with different porosities were fabricated using the optimized processing conditions of laser power, scanning speed, and hatching pattern. In this process micro-CT images of the structure of cancellous bone were stored in a computer and modified a little due to certain limitations of this method. For example, wall thicknesses of less than 200 μm are difficult to process and, hence, the wall thickness was increased to more than 300 μm. In this process specimens were always prepared from the bottom to the top.

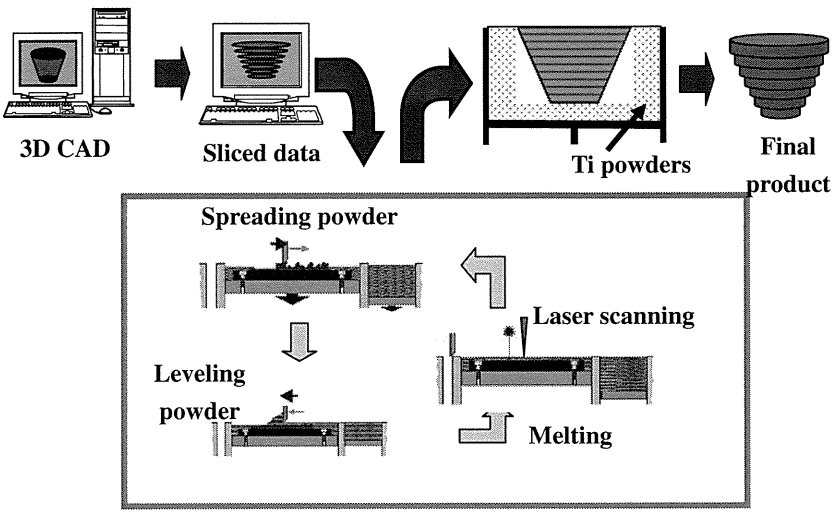

Fig. 1. Schematic representation of the SLM process.